

UNIVERSITÉ DU QUÉBEC À MONTRÉAL

LES CARACTÉRISTIQUES DE LA NEIGE ET LA RÉTROACTION DE  
L'ALBÉDO DE LA NEIGE EN AMÉRIQUE DU NORD SIMULÉES PAR LE  
MODÈLE RÉGIONAL CANADIEN DU CLIMAT (MRCC5)

MÉMOIRE PRÉSENTÉ  
COMME EXIGENCE PARTIELLE  
DE LA MAÎTRISE EN SCIENCES DE L'ATMOSPHÈRE

PAR

BRUNO FANG

MAI 2016

UNIVERSITÉ DU QUÉBEC À MONTRÉAL  
Service des bibliothèques

Avertissement

La diffusion de ce mémoire se fait dans le respect des droits de son auteur, qui a signé le formulaire *Autorisation de reproduire et de diffuser un travail de recherche de cycles supérieurs* (SDU-522 – Rév.07-2011). Cette autorisation stipule que «conformément à l'article 11 du Règlement no 8 des études de cycles supérieurs, [l'auteur] concède à l'Université du Québec à Montréal une licence non exclusive d'utilisation et de publication de la totalité ou d'une partie importante de [son] travail de recherche pour des fins pédagogiques et non commerciales. Plus précisément, [l'auteur] autorise l'Université du Québec à Montréal à reproduire, diffuser, prêter, distribuer ou vendre des copies de [son] travail de recherche à des fins non commerciales sur quelque support que ce soit, y compris l'Internet. Cette licence et cette autorisation n'entraînent pas une renonciation de [la] part [de l'auteur] à [ses] droits moraux ni à [ses] droits de propriété intellectuelle. Sauf entente contraire, [l'auteur] conserve la liberté de diffuser et de commercialiser ou non ce travail dont [il] possède un exemplaire.»



## REMERCIEMENTS

Je désire remercier ma directrice de recherche, Dr. Laxmi Sushama, pour avoir dirigé mon projet et mon directeur de programme, Dr. René Laprise, pour avoir amélioré mes aptitudes en communication.

Je tiens également à remercier les membres du centre ESCER pour leur contribution à mon développement académique et professionnel. Un remerciement distingué est dédié à Dr. Gulilat Tefera Diro, Katja Winger et Arlette Chacon qui m'ont aidé en programmation informatique.

Enfin, j'aimerais souligner la présence de mes collègues de bureau pour leur support moral et Gregory Yang pour sa grande amitié dans cette aventure.



## TABLE DES MATIÈRES

REMERCIEMENTS .....	III
LISTE DES FIGURES.....	VII
LISTE DES TABLEAUX.....	IX
LISTE DES ACRONYMES .....	XI
LISTE DES SYMBOLES .....	XIII
RÉSUMÉ.....	XV
CHAPITRE I	
INTRODUCTION.....	1
1.1 Motivation .....	1
1.2 Objectifs .....	3
1.3 Méthodologie .....	3
CHAPITRE II	
SNOW CHARACTERISTICS AND SNOW ALBEDO FEEDBACK OVER NORTH AMERICA AS SIMULATED BY THE CANADIAN REGIONAL CLIMATE MODEL.....	9
Abstract .....	10
2.1 Introduction .....	12
2.2 Model description.....	14
2.3 Methods and data .....	17
2.4 Results .....	20
2.4.1 Validation .....	20
2.4.2 Projected changes.....	23
2.4.3 CAT in the climate change context.....	25
2.4.4 $\partial\alpha_p / \partial\alpha_s$ and SAF strength .....	26
2.5 Conclusions .....	27
CHAPITRE III	

DISCUSSION DES RÉSULTATS ET CONCLUSIONS .....	47
RÉFÉRENCES.....	53

## LISTE DES FIGURES

Figures	Pages
Figure 2.1: (a) Mean 2-m air temperature from CRU (first column), difference between CRCM5 driven by ERA-40/ERA-Interim and CRU (second column), difference between CRCM5 driven by CanESM2 and CRCM5 driven by ERA-40/ERA-Interim (third column), and difference between CRCM5 driven by MPI-ESM and CRCM5 driven by ERA-40/ERA-Interim (fourth column), for the 1976-2009 period. (b) Same as in (a) but for precipitation rate for the 1998-2008 period. ....	32
Figure 2.2: (a) Mean snow depth from CMC (first column), difference between CRCM5 driven by ERA-40/ERA-Interim and CMC (second column), difference between CRCM5 driven by CanESM2 and CRCM5 driven by ERA-40/ERA-Interim (third column), and difference between CRCM5 driven by MPI-ESM and CRCM5 driven by ERA-40/ERA-Interim (fourth column), for the 1979-1997 period. (b) Same as in (a) but for SWE. ....	33
Figure 2.3: Model simulated and observed annual cycle of (a) snow depth, (b) SWE, and (c,d) surface albedo for a part of the midlatitude regions ( $115^{\circ}\text{W}$ - $55^{\circ}\text{W}$ , $40^{\circ}\text{N}$ - $65^{\circ}\text{N}$ ). (a) and (b) correspond to the 1979-1997 period, (c) and (d) correspond to the 1984-2000 and 2001-2010 periods, respectively. CRCM5 driven by ERA-40/ERA-Interim is in a black line, CRCM5 driven by CanESM2 is in a green line, CRCM5 driven by MPI-ESM is in a blue line, and observation is in a red line. ....	34
Figure 2.4: (a) Mean snow cover from MODIS (first column), difference between CRCM5 driven by ERA-40/ERA-Interim and MODIS (second column), difference between CRCM5 driven by CanESM2 and CRCM5 driven by ERA-40/ERA-Interim (third column), and difference between CRCM5 driven by MPI-ESM and CRCM5 driven by ERA-40/ERA-Interim (fourth column), for the 2001-2010 period. (b) Same as in (a) but for snow albedo. ....	35
Figure 2.5: Mean surface albedo from (a) ISCCP (first column), difference between CRCM5 driven by ERA-40/ERA-Interim and ISCCP (second column), difference between CRCM5 driven by CanESM2 and	

CRCM5 driven by ERA-40/ERA-Interim (third column), and difference between CRCM5 driven by MPI-ESM and CRCM5 driven by ERA-40/ERA-Interim (fourth column), for the 1984-2000 period.	36
(b) Same as in (a) but for MODIS for the 2001-2010 period. ....	36
Figure 2.6: Change in surface albedo associated with surface air temperature change (first column; % K <sup>-1</sup> ), snow cover feedback (second column; % K <sup>-1</sup> ), and air temperature dependence of snow albedo (third column; % K <sup>-1</sup> ) in the seasonal cycle context between May and April of the 2001-2010 period, from CRCM5 driven by ERA-40/ERA-Interim (first row) and MODIS (second row). ....	37
Figure 2.7: Projected changes to snow cover (first column; %), snow albedo (second column; %), and surface albedo (third column; %), for the 2071-2100 MAM period with respect to the 1976-2005 MAM period. CRCM5 driven by CanESM2 RCP 4.5 (first row), CRCM5 driven by CanESM2 RCP 8.5 (second row), CRCM5 driven by MPI-ESM RCP 4.5 (third row), and CRCM5 driven by MPI RCP 8.5 (fourth row). Grid points with no snow are masked in grey in the middle column. ....	38
Figure 2.8: Change in surface albedo associated with air temperature change (first column; % K <sup>-1</sup> ), snow cover feedback (second column; % K <sup>-1</sup> ), and air temperature dependence of snow albedo (third column; % K <sup>-1</sup> ) in the climate change context between the 2071-2100 MAM period and the 1976-2005 MAM period. ....	39
Figure 2.9: Air temperature dependence of snow albedo (first column; % K <sup>-1</sup> ), snow albedo changes (second column; %), and snowfall occurrence changes (third column; days) in the seasonal cycle context (first row) and in the climate change context (second row), based on CRCM5 driven by ERA-40/ERA-Interim and CRCM5 driven by CanESM2 RCP 4.5. ....	40
Figure 2.10: Variation in planetary albedo with surface albedo (top) and SAF strength (bottom; W m <sup>-2</sup> K <sup>-1</sup> ) in the seasonal cycle context (first column) and in the climate change context (second, third, fourth and fifth column), based on CRCM5 driven by ERA-40/ERA-Interim, CRCM5 driven by CanESM2 for RCP 4.5 and 8.5, and CRCM5 driven by MPI-ESM for RCP 4.5 and 8.5. ....	41

## LISTE DES TABLEAUX

Tableau	Page
Tableau 2.1 : The five CRCM5 simulations used in this study (first column), the corresponding simulation periods (second column), driving data (third column), and analysis periods (fourth column). .....	44



## LISTE DES ACRONYMES

BRDF	Bi-directional Reflectance Distribution Function
CanESM2	2 <sup>nd</sup> version of the Canadian Earth System Model
CAT	Change in Surface Albedo Associated with an Increase in Surface Air Temperature
CLASS	Canadian Land Surface Scheme
CMC	Canadian Meteorological Centre
CMIP3	Coupled Model Intercomparison Project Phase 3
CMIP5	Coupled Model Intercomparison Project Phase 5
CRCM5	fifth-generation of the Canadian Regional Climate Model
CRU	Climate Research Unit
DISORT	Discrete-Ordinate Radiative Transfer
DJF	December, January and February
ECMWF	European Centre for Medium-Range Weather Forecasts
ERA	European Centre for Medium-Range Weather Forecasts Re-Analysis
GCM	General Circulation Model
GEM	Global Environment Multiscale
GIEC	Groupe d'experts Intergouvernemental sur l'Évolution du Climat
GISS	Goddard Institute for Space Studies
IPCC AR4	Fourth Assessment of the Intergovernmental Panel on Climate Change
ISCCP	International Satellite Cloud Climatology Project

MAM	March, April and May
MCG	Modèle de Circulation Générale
MRCC5	5 <sup>e</sup> version du Modèle Régional Canadien du Climat
MODIS	Moderate-Resolution Imaging Spectroradiometer
MPI-ESM	Max Planck Institute Earth System Model
NDSI	Normalized Difference Snow Index
PIMC5	Phase 5 du Projet d'Intercomparaison de Modèle Couplé
RCP	Representative Concentration Pathway
SAF	Snow Albedo Feedback
SCF	Snow Cover Feedback
SWE	Snow Water Equivalent
TDA	Temperature Dependence of Snow Albedo
TOA	Top of the Atmosphere

## LISTE DES SYMBOLES

$Q_{TOA}^{in}$	Incoming shortwave radiation at the TOA
$Q_{TOA}^{net}$	Net shortwave radiation at the TOA
$T_s$	Surface air temperature
$S_c$	Snow cover
$\alpha_s$	Surface albedo
$\alpha_p$	Planetary albedo
$\alpha_{snow}$	Snow albedo
$\alpha_{land}$	Land albedo



## RÉSUMÉ

La rétroaction de l'albédo de la neige augmente la sensibilité du climat des continents de l'hémisphère nord et diverge largement entre les modèles de climat. Cette étude vise donc à évaluer les caractéristiques de la neige et la rétroaction de l'albédo de la neige en Amérique du Nord dans la cinquième génération du Modèle Régional Canadien du Climat (MRCC5). La force de rétroaction de l'albédo de la neige est définie par le gain en rayonnement solaire net au sommet de l'atmosphère lorsqu'il y a une diminution d'albédo associé à une augmentation de température à la surface. Cette force est contrôlée par un terme d'atmosphère défini par la variation de l'albédo planétaire avec la surface, et par un terme de surface défini par le changement de l'albédo de la surface associé à une augmentation de température à la surface. Ce dernier est déterminé par la somme d'une rétroaction de la couverture neigeuse et d'une dépendance de l'albédo de la neige à la température. Dans cette étude, les caractéristiques de la neige et le terme de surface de la rétroaction de l'albédo de la neige dans le cycle saisonnier sont validés en comparant une simulation du MRCC5 pilotée par les réanalyses ERA-40 et ERA-Interim avec les observations disponibles. Les changements projetés des caractéristiques de la neige sont évalués pour la période de 2071-2100 par rapport à la période de 1976-2005 avec des simulations de changement climatique transitoire pilotées par CanESM2 et MPI-ESM, pour les RCP 4.5 et 8.5. Étant donné l'importance d'évaluer les erreurs dans les simulations issues des erreurs de données de pilotage, les erreurs de conditions aux frontières sont également évaluées en comparant les simulations pilotées par les MCGs avec celle pilotée par ERA-40/ERA-Interim. De plus, le terme de surface de la rétroaction de l'albédo de la neige est évalué dans un contexte de changement climatique.

La validation suggère que le modèle est en mesure de représenter la distribution spatiale de la profondeur et de l'équivalent en eau de la neige dans les latitudes moyennes, mais une surestimation est observée dans l'archipel arctique canadien. L'albédo de la neige du MRCC5 est surestimé dans les forêts et les montagnes des latitudes moyennes, comparé aux observations. Il faut noter qu'il peut aussi y avoir des incertitudes considérables dans les observations. Les résultats indiquent que le terme de surface de la rétroaction de l'albédo de la neige dans le MRCC5 est surestimé et presqu'entièrement contrôlé par la rétroaction de la couverture neigeuse alors que pour les observations tel que le Moderate-Resolution Imaging Spectroradiometer (MODIS), la rétroaction de la couverture neigeuse et la dépendance de l'albédo de la neige à la température ont des forces plus ou moins similaires. La surestimation du terme de surface de la rétroaction de l'albédo de la

neige semble être liée à la rétroaction de la couverture neigeuse, qui est directement liée à l'albédo de la neige. Ceci indique qu'une amélioration de la représentation de l'albédo de la neige est nécessaire dans le modèle.

Mots clés : caractéristiques de la neige; rétroaction de l'albédo de la neige; Modèle Régional Canadien du Climat; validation; changement climatique





# CHAPITRE I

## INTRODUCTION

### 1.1 Motivation

Durant les dernières décennies, le réchauffement observé en Arctique est environ deux fois plus grand que le réchauffement global moyen (Solomon et al. 2007). La rétroaction de l'albédo de la neige est bien connue pour être un facteur important dans ce réchauffement arctique, particulièrement au printemps. De nombreux études (Qu and Hall 2006, et les références reliées) se sont donc concentrées à évaluer la force de rétroaction de l'albédo de la neige, définie par le gain en rayonnement solaire net au sommet de l'atmosphère lorsqu'il y a une diminution d'albédo associé à une hausse de température à la surface (Hall 2004). La force de rétroaction de l'albédo de la neige est contrôlée par deux facteurs. Le premier est une variation de l'albédo planétaire par rapport à l'albédo de la surface. Le deuxième, relié exclusivement aux processus en surface, est un changement de l'albédo de la surface associé à une hausse de température à la surface (CAT). Ce dernier peut lui-même se décomposer en deux autres termes de rétroaction positives. Le premier terme est un contraste de l'albédo entre une surface couverte de neige et une surface sans neige, appelé la rétroaction de la couverture neigeuse (SCF). Une hausse de température à la surface engendre une diminution de la couverture neigeuse et de l'albédo de la surface. Par conséquent, la surface absorbe plus de rayonnement solaire et se réchauffe davantage. Le deuxième terme est une dépendance de l'albédo de la neige à la température (TDA), aussi appelé la rétroaction de la métamorphose

dans certains articles. Il faut noter que la neige fondante possède un albédo plus bas que la neige gelée (Robock 1980). Une hausse de la température à la surface diminue directement l'albédo de la neige par les propriétés de vieillissement de la neige. Encore une fois, la surface absorbe plus de rayonnement solaire et se réchauffer davantage.

En utilisant les Modèles de Circulation Générales (MCGs) du 4<sup>ième</sup> rapport du Groupe d'experts Intergouvernemental sur l'Évolution du Climat (GIEC), Hall et Qu (2006) ont montré qu'il y a une divergence triple du CAT sans de préférence précise vers une valeur centrale. Cette divergence a continué à persister dans les modèles de la Phase 5 du Projet d'Intercomparaison de Modèle Couplé (PIMC5) (Hall and Qu 2014) et les auteurs croient qu'elle est associée à la représentation de l'albédo de la neige et le masquage de la neige sur la végétation (Hall and Qu 2007, Loranty et al. 2014). Qu et Hall (2006) ont également démontre que le CAT dans le contexte du cycle saisonnier constitue un bon prédicteur pour le CAT dans le contexte du changement climatique étant donné leur forte corrélation. Par conséquent, on s'attend à ce qu'une réduction des erreurs du CAT dans le cycle saisonnier puisse réduire les erreurs du CAT dans le changement climatique. Ceci dit, les observations satellitaires constituent un besoin important pour contraindre le CAT dans les modèles climatiques. Les études basées sur les MCGs du 4<sup>ième</sup> rapport du GIEC et de la Phase 3 du Projet d'Intercomparaison de Modèle Couplé (PIMC3) montrent que le CAT est contrôlé par la SCF (Hall and Qu 2007, Fletcher et al. 2012). Dans les observations, la SCF et la TDA ont des contributions similaires sur le CAT, avec une plus grande correlation du CAT avec la SCF, mais pas aussi grande que celle évaluée avec les MCGs (Fernandes, Zhao, Wang, Key, Qu and Hall 2009). En ce qui concerne la distribution spatiale, la SCF domine les régions sous la latitude de 65°N alors que la TDA domine les régions arctiques. La comparaison entre les modèles montre que le CAT peut bel et bien être expliquée par la somme de la SCF et la TDA.

## 1.2 Objectifs

Le but de cette étude est d'évaluer les caractéristiques de la neige et la rétroaction de l'albédo de la neige en Amérique du Nord avec la cinquième génération du Modèle Régional Canadien du Climat (MRCC5). L'étude se concentre sur les mois printaniers de l'hémisphère nord car c'est durant cette période que le CAT dans les simulations de changement climatique global est le plus fort (Hall 2004). La profondeur de la neige, l'équivalent en eau de la neige, la couverture neigeuse, l'albédo de la neige et l'albédo de la surface, simulés par le modèle piloté par les réanalyses, sont validés avec les observations disponibles. Le CAT dans le cycle saisonnier, simulé par le modèle, est également validé avec des observations satellitaires. Les changements projetés des caractéristiques de la neige sont évalués avec les simulations de changement climatique transitoire du MRCC5 pilotées par deux MCGs, pour les scénarios de forçage anthropique RCPs 4.5 et 8.5 (Taylor et al. 2012). Les erreurs de conditions aux frontières sont aussi évaluées en comparant ces simulations pilotées par les MCGs avec la simulation pilotée par les réanalyses pour le climat présent. Enfin, ces simulations de changement climatique sont utilisées pour évaluer le CAT dans le contexte de changement climatique. La représentation adéquate des caractéristiques de la neige et de la rétroaction de l'albédo de la neige est importante pour avoir de meilleures simulations du climat régional et de l'hydrologie du climat présent et futur.

## 1.3 Méthodologie

### 1.3.1 Description du modèle et des simulations

Le MRCC5 (Zadra et al. 2008) est basé sur une version du Global Environment Multiscale (GEM) pour un domaine limité. Le MRCC5 est utilisé dans de nombreuses études sur différentes régions à travers le monde. Il est également utilisé dans plusieurs applications hydrologiques. Jusqu'à présent, l'équivalent en eau de la neige est la seule caractéristique de la neige validée dans le MRCC5. Donc pour la première fois, cette étude valide les autres caractéristiques de la neige tels que la profondeur de la neige, la couverture neigeuse, l'albédo de la neige ainsi que la rétroaction de l'albédo de la neige.

La neige est modélisé par le schéma de surface du MRCC5, soit le Canadian Land Surface Scheme (CLASS 3.5) (Verseghy 2009). Le CLASS modélise la neige sur une couche unique dans laquelle le vieillissement de la neige, l'accumulation de la neige et la fonte de la neige sont paramétrés. La couverture neigeuse est égale à 1 lorsque la profondeur de la neige est plus grande ou égale à 0.10 m. Si la profondeur de la neige est plus petite que 0.10 m, la couverture neigeuse est proportionnelle à la profondeur de la neige avec un coefficient de proportionnalité choisie comme étant l'inverse du seuil de 0.10 m. Le vieillissement de la neige est représenté par une augmentation de la densité de la neige et une diminution exponentielle de l'albédo de la neige. La densité de la neige augmente exponentiellement avec le temps d'une valeur pour une couche de neige fraîche à une valeur de fond pour une couche de neige vieille (Longley 1960, Gold 1958). L'albédo de la neige diminue exponentiellement avec le temps de 0.84 pour une couche de neige fraîche à une valeur pour une couche de neige vieille (Aguado 1985, Robinson and Kukla 1984, Dirmhirn and Eaton 1975). En cas d'une chute de neige, la densité de la neige est ajusté comme étant la moyenne pondérée de la densité de la nouvelle neige et la densité de la neige précédente. De plus, l'albédo de la neige retourne de nouveau à 0.84. La fonte de la neige se produit lorsque la température de la couche dépasse 0 °C. Ce dernier peut se produire soit à partir de l'équilibre énergétique de la surface ou soit à partir de la conduction de la chaleur de la couche sous-jacente. L'interception et le relâchement de la neige de la canopée sont modélisés en suivant la méthode de

Hedstrom and Pomeroy (1998). À chaque pas de temps, la quantité de neige intercepté lors d'une chute de neige est obtenu en fonction de la quantité de neige incidente sur la canopée lors de ce pas de temps, la quantité de neige initiale interceptée et la capacité d'interception. Le taux de relâchement de la neige est estimé à partir d'une fonction exponentielle empirique avec un coefficient de relâchement d'une valeur de  $0.1 \text{ d}^{-1}$  ou  $1.157 \times 10^{-6} \text{ s}^{-1}$ .

Dans cette étude, cinq simulations du MRCC5 sont considérées, couvrant le domaine de l'Amérique du Nord sur une résolution horizontale de  $0.44^\circ$ . La première simulation est pilotée par les réanalyses ERA-40 (Uppala et al. 2005) pour la période de 1958 à 1978 et ERA-Interim (Dee et al. 2011) pour la période de 1979 à 2014 du European Centre for Medium-range Weather Forecasting (ECMWF). Les quatre autres simulations sont des simulations de changement climatique transitoire pour la période de 1950 à 2100. Elles sont pilotées par la deuxième génération du Canadian Earth System Model (CanESM2) (Arora et al. 2011) et par le Max Planck Institute Earth System Model (MPI-ESM) (Giorgetta et al. 2013), en utilisant deux scénarios de forçage anthropique partant de l'année 2006, RCPs 4.5 et 8.5 (Taylor et al. 2012).

### 1.3.2 Validation

Une étude des erreurs de performance, c.-à-d. les erreurs due à la physique et à la dynamique du modèle, est effectuée en comparant caractéristiques de la neige simulée par le MRCC5 piloté par les réanalyses ERA-40/ERA-Interim avec les observations disponibles pour les saisons de l'hiver (DJF) et du printemps (MAM). Tout d'abord, la température à 2 mètre et la précipitation du MRCC5 seront comparées avec celles du Climate Research Unit (CRU). Les observations sur grille du CRU TS3.10 seront utilisées pour effectuer la validation. Ce produit provient des observations mensuelles des stations météorologiques sur les régions continentales à travers le monde qui sont interpolées sur une résolution de  $0.5^\circ$  pour la période de 1961 à 2009 (Mitchell and Jones 2005).

Les observations de la profondeur et l'équivalent en eau de la neige sont fournis par le Canadian Meteorological Centre (CMC) (Brown et al. 2003) sur une fréquence journalière et sur une résolution de  $0.25^\circ$  pour la période de 1979 à 1997. Ce produit est développé à partir des données de profondeur de la neige mesurée à la règle dans les stations météorologiques à travers le Canada et les États-Unis. Le champ d'essai a été généré à partir d'un modèle de représentation de la densité de la neige piloté par des valeurs de température de l'air et de précipitation provenant des réanalyses ERA-15. Ce modèle paramétrise des processus tels que l'accumulation de la neige, le vieillissement de la neige et la fonte de la neige. Une estimation de l'équivalent en eau de la neige est également fournie à partir de la profondeur et de la densité de la neige.

La couverture neigeuse et l'albédo de la neige observés sont fournis par les satellites du Moderate-Resolution Imaging Spectroradiometer (MODIS), sous un produit nommé MOD10A1. Le radiomètre de MODIS capte des radiances dans 36 bandes entre les longueurs d'onde de  $0.412 \mu\text{m}$  à  $14.235 \mu\text{m}$  (Barnes et al. 1998). Les données de couverture neigeuse et d'albédo de la neige sont journalières et possèdent une résolution de 500 m. Pour déterminer la couverture neigeuse, MODIS utilise un algorithme basé sur l'indice de neige par différence normalisée (Riggs et al. 2006) et pour déterminer l'albédo de la neige, il utilise une fonction de distribution de la réflectance bidirectionnelle pour la neige (Stroeve et al. 2002 ; Stroeve et al. 2006) basé sur un modèle de transfert radiatif discrète-ordonnée (Stamnes et al. 1998).

Enfin, les produits d'observations satellitaires ISCCP-FD du International Satellite Cloud Climatology Project (ISCCP) et MCD43C3 du MODIS seront utilisés pour valider l'albédo de la surface. Le ISCCP-FD (Zhang et al. 2004) fournit des données mensuelles de rayonnement solaire entrant et sortant sur une grille de  $2.5^\circ$  pour la période de 1984 à 2000, avec lesquelles les valeurs d'albédo de la surface sont calculés. Ce produit est réalisé à partir du modèle de transfert radiatif de la NASA Goddard Institute for Space Studies (Hansen et al. 2002 ; Oinas et al. 2001) ainsi que

des données ISCCP D1 (Rossow and Schiffer 1999) provenant de plusieurs satellites en orbite polaire et géostationnaire. Ces satellites captent des radiances dans le domaine du visible ( $\sim 0.6 \mu\text{m}$ ), de l'infrarouge proche ( $\sim 3.7 \mu\text{m}$ ) et de l'infrarouge moyen ( $\sim 11 \mu\text{m}$ ) dans le but de calculer des variables caractéristiques des nuages. Le MCD43C3 fournit des données d'albédo de la surface aux 8 jours sur une résolution de  $0.05^\circ$  en employant la fonction de distribution de la réflectance bidirectionnelle (Wanner et al. 1995). Ce produit est une combinaison des données récoltées par les satellites Terra et Aqua de MODIS (Barnes et al. 1998) pour la période de 2001 à 2010.

En suivant la méthode de Hall et Qu (2007), la composante de la surface de la force de rétroaction de l'albédo de la neige, définie par le CAT, est calculée par la somme de la SCF et TDA. Pour la validation, ces termes seront évalués dans le contexte du cycle saisonnier en utilisant les mois d'avril et mai de la période de 2001 à 2010. Ils seront calculés d'une part, avec la simulation du MRCC5 pilotée par ERA-40/ERA-Interim et d'autre part, avec les observations satellitaires de MODIS et les réanalyses d'ERA-Interim pour la température.

### 1.3.3 Changements projetés

Les changements projetés des caractéristiques de la neige tels que la couverture neigeuse, l'albédo de la neige et l'albédo de la surface seront calculés pour la période de 2071-2100 par rapport à la période de 1976-2005. Les simulations de changement climatique transitoire sont pilotées par CanESM2 et MPI-ESM, pour les RCPs 4.5 et 8.5. Avant tout, les erreurs de conditions aux frontières pour ces variables, c.-à-d. les erreurs générées par les données de pilotage, seront analysées en comparant les simulations du MRCC5 pilotées par CanESM2 et MPI-ESM avec la simulation pilotée par ERA-40/ERA-Interim pour le climat présent.

### 1.3.4 CAT dans un changement climatique

Le CAT, la SCF et la TDA seront évalués dans le contexte du changement climatique en utilisant les mêmes périodes et les mêmes simulations que dans les changements projetés des caractéristiques de la neige. Une comparaison de ces quatre simulations permettra de déterminer la sensibilité de ces termes par rapport aux données de pilotage ainsi qu'aux scénarios RCPs. Enfin, les cinq simulations du MRCC5 seront également utilisées pour calculer le premier terme  $\partial\alpha_p/\partial\alpha_s$  et la force de rétroaction de l'albédo de la neige dans les contextes du cycle saisonnier et du changement climatique.

#### Organisation du mémoire :

Pour commencer, le chapitre I est une introduction du mémoire répartie en trois sections : 1.1 Motivation, 1.2 Objectifs et 1.3 Méthodologie. Le chapitre II est un article en anglais prêt pour une soumission à un journal scientifique. Cet article est réparti en cinq sections : 2.1 Introduction, 2.2 Description du modèle, 2.3 Méthode et données, 2.4 Résultats, 2.5 Conclusion. Le chapitre III est une discussion des résultats et les conclusions du mémoire.

## CHAPITRE II

### SNOW CHARACTERISTICS AND SNOW ALBEDO FEEDBACK OVER NORTH AMERICA AS SIMULATED BY THE CANADIAN REGIONAL CLIMATE MODEL

Bruno Fang<sup>1\*</sup>, Laxmi Sushama<sup>1</sup>, Gulilat Tefera Diro<sup>1</sup>, Patrick Samuelsson<sup>2</sup>, Diana Verseghy<sup>1,3</sup>, Stephen J. Déry<sup>4</sup>

<sup>1</sup>Centre ESCER (Étude et Simulation du Climat à l'Échelle Régionale), Université du Québec at Montréal, Montréal, Québec, Canada

<sup>2</sup>Swedish Meteorological and Hydrological Institute, Norrköping, Östergötland, Sweden

<sup>3</sup>Climate Research Division, Environment Canada and Climate Change, Toronto, Ontario, Canada

<sup>4</sup>University of Northern British Columbia, Prince George, British Columbia, Canada

\*Corresponding author  
Tel : +1 514-987-3000 ext. 2414  
Fax : +1 514-987-6853  
Email : fang.bruno@courrier.uqam.ca

(To be submitted to Climate Dynamics)

## Abstract

This study focuses on the validation of snow characteristics and snow albedo feedback (SAF) and its surface and atmospheric components, in a seasonal cycle context, within a fifth-generation Canadian Regional Climate Model (CRCM5) simulation driven by reanalysis, over North America. The surface component of SAF is determined here as the sum of a snow cover feedback term and a term representing the temperature dependence of snow albedo, while the atmospheric component is determined as the change in planetary albedo with surface albedo. Projected changes to snow characteristics for the 2071–2100 period with respect to the 1976–2005 period are then assessed based on two CRCM5 transient climate change simulations driven by two different Coupled Model Intercomparison Project Phase 5 (CMIP5) Global Climate Models (GCMs), for Representative Concentration Pathways (RCPs) 4.5 and 8.5. The surface and atmospheric components of SAF are also assessed in the climate change context.

Validation results suggest that CRCM5 is able to represent the main spatial and temporal patterns of snow depth and snow water equivalent over the midlatitude regions, but some overestimation is noted over the high-latitude regions, when compared with the Canadian Meteorological Centre dataset. Snow albedo is overestimated in CRCM5 over the boreal forests and the midlatitude regions with important orography, in comparison with the Moderate-Resolution Imaging Spectroradiometer (MODIS) data. Furthermore, CRCM5 underestimates the temperature dependence of snow albedo and highly overestimates the snow cover feedback term compared to MODIS, which overall lead to an overestimation of the surface component of SAF. This overestimation appears to be linked primarily to the simulated snow albedo, which suggests that improvements to the representation of snow albedo are required in the model. SAF in the climate change context agrees with that estimated for the seasonal cycle context in that the snow cover feedback is the

dominant of the two terms controlling the surface component of SAF. Important differences in the spatial patterns, particularly those associated with maximum values, for the snow cover feedback and temperature dependent snow albedo terms are noted between the climate change and seasonal cycle contexts, and SAF appears to be more sensitive to the driving data.

*Keywords :* snow characteristics; snow albedo feedback; North America; Canadian Regional Climate Model; validation; climate change

## 2.1 Introduction

The observed Arctic warming during the recent decades is about two times greater than the global average warming (Solomon et al. 2007), and the snow albedo feedback (SAF) is an important process contributing to this Arctic amplification, particularly during the spring season. A number of studies (Qu and Hall 2006, Thackeray and Fletcher 2016, and the references therein) have focussed on assessing the strength of SAF, which is defined as the amount of additional net shortwave radiation at the top of the atmosphere (TOA) as surface albedo decreases in association with an increase in surface air temperature (Hall 2004). As demonstrated in Qu and Hall (2006), the strength of SAF is controlled by two factors. The first factor is the variation in planetary albedo with surface albedo, which represents the attenuation effect of the atmosphere on surface albedo changes. The second factor, related exclusively to surface processes, is the change in surface albedo associated with an increase in surface air temperature (CAT). This second factor can be further decomposed into two positive feedback terms. The first term is due to the albedo contrast between snow covered and snow-free land, referred to as the snow cover feedback (SCF). The second term is the temperature dependence of snow albedo (TDA), also referred to as metamorphosis feedback in some articles (Hall and Qu 2007, Fernandes et al. 2009), and is the result of lower albedo values of wet melting snow compared to dry snow (Robock 1980).

Using global climate models (GCMs) from the Fourth Assessment of the Intergovernmental Panel on Climate Change (IPCC AR4), Hall and Qu (2006) have shown that there is a large spread in CAT, without a clear preference towards a central value. This spread has continued to persist in the Coupled Model Intercomparison Project Phase 5 (CMIP5) GCMs (Hall and Qu 2014), and is believed to be associated with the inadequate representations of snow albedo and the snow-masking effect of vegetation (Hall and Qu 2007, Essery 2013, Loranty et al. 2014,). Furthermore, Hall and Qu (2006) have shown that simulated CAT in the seasonal

cycle context is a good predictor for that in the climate change context because of their strong correlation. Hence, it can be expected that a reduction of errors in CAT for the seasonal cycle will reduce errors in that for the climate change. That said, there is a need for satellite based observations to constrain CAT in climate models. Studies based on GCMs from the IPCC AR4 and the Coupled Model Intercomparison Project Phase 3 (CMIP3) have shown that simulated CAT is mostly controlled by SCF (Qu and Hall 2007, Fletcher et al. 2012). However, in satellite data, the strength of observed SCF and TDA are similar, with a higher correlation of CAT with the SCF (Fernandes et al. 2009). Furthermore, the observed SCF dominates equatorward of 65°N whereas TDA dominates the Arctic regions. The comparison between models indicate that the approximate sum of SCF and TDA fully explains CAT when the three terms are calculated separately (Fletcher et al. 2012). Letcher and Minder (2015) recently demonstrated the added value of high-resolution simulations in the estimation of SAF by comparing regional climate model simulations at 36 km, 12 km and 4 km resolutions over a complex terrain. They obtained significant differences between simulated SAF at 36 km resolution and that at 12 and 4 km resolution, due to the inadequate representation of snow accumulation and ablation due to terrain smoothing.

The goal of this paper is to assess snow characteristics and SAF simulated by the fifth-generation of the Canadian Regional Climate Model (CRCM5) over the North American landmass. Most of the studies so far have focussed on either CAT in GCMs using the explicit contributions of SCF and TDA, or on CAT in regional climate models using simply surface albedo and surface air temperature. This study presents for the first time a systematic analysis of the contribution of SCF and TDA to CAT in a regional climate model and MODIS dataset. The assessment is focused on Northern Hemisphere (NH) spring because CAT in simulated global climate change is strongest during that period (Hall 2004). Snow depth, snow water equivalent (SWE), snow cover, snow albedo, and surface albedo are validated by

comparing reanalysis-driven CRCM5 simulations with available observations. CAT in the seasonal cycle context is also validated by comparing with satellite observations. Projected changes to snow characteristics are assessed using CRCM5 transient climate change simulations driven by two GCMs, for two Representative Concentration Pathways (RCPs) (Taylor et al. 2012). The boundary forcing errors are also assessed by comparing these GCM driven simulations with reanalysis driven simulation for the current period. Furthermore, the climate change simulations are used to evaluate CAT in the climate change context. Capturing these snow characteristics and SAF components adequately is important to ensure better simulation of the regional climate and the hydrology in current and future climates.

## 2.2 Model description

The model used in this study is CRCM5 (Zadra et al. 2008), which is based on a limited-area version of the Global Environment Multiscale (GEM) model used for numerical weather prediction at Environment and Climate Change Canada (Côté et al. 1998). GEM employs semi-Lagrangian transport and a (quasi) fully implicit stepping scheme. It also uses a vertical coordinate based on hydrostatic pressure in a fully elastic non-hydrostatic formulation (Laprise 1992). CRCM5 contains the following physical parameterizations inherited from GEM: a deep convection scheme following Kain and Fritsch (1990), shallow convection based on a transient version of the Kuo (1965) scheme (Bélair et al. 2005), large-scale condensation (Sundqvist et al. 1989), correlated-K solar and terrestrial radiation (Li and Barker 2005), and subgrid low-level orographic gravity-wave drag (McFarlane 1987). The planetary boundary layer is represented following Benoit et al. (1989), Delage and Girard (1992), and Delage (1997) with some modifications as discussed in Zadra et al. (2012). The low-level orographic blocking parameterization of Zadra et al. (2003)

is employed, again with some modifications as reported in Zadra et al. (2012). Lakes are represented in CRCM5 by the Flake model described in Mironov et al. (2010).

The land surface scheme used in CRCM5 is a fairly recent version of the Canadian Land Surface Scheme (CLASS 3.5) (Verseghy 2009). CLASS allows flexible soil layer and depth configurations and includes prognostic equations for energy and water content of the soil layers. This land surface scheme models the snowpack as thermally and hydrologically distinct from the underlying soil. To represent variability at the subgrid-scale, CLASS uses a pseudomosaic approach by dividing the land fraction of each grid cell into four subareas: bare soil, vegetation, snow over bare soil, and snow with vegetation. The energy and water budget equations are first solved for each subarea separately and then averaged over the grid cell. Vegetation is modelled using averaged structural attributes and physiological properties of the four broad plant functional types simulated in CLASS. The structural attributes include leaf area index, roughness length, canopy mass and root depth. The four plant functional types consist of needleleaf and broadleaf trees, crops and grass. In this study, the fractional areas of plant functional types are prescribed from ECOCLIMAP (Masson et al. 2003) and soil texture is prescribed from the United States Geology Survey (USGS).

In CLASS, snow is modelled as a single variable thickness layer, where snow ageing, snow accumulation, and snow melting are parameterized. Snow cover is assumed to be 1 if the snow depth is greater than or equal to 0.10 m. If the calculated snow depth is less than 0.10 m, the snow cover is re-evaluated as the snow depth divided by the 0.10 m threshold and the snow depth is reset to 0.10. CLASS represents snow ageing as an increase in snow density and decrease in snow albedo. Snow density increases exponentially with time from a fresh snow value to a background old snow density, based on an empirical expression from Longley (1960) and Gold (1958). Snow albedo decreases exponentially with time from a fresh snow value of 0.84 to a background old snow value, following an expression based on data given in Aguado (1985), Robinson and Kukla (1984), and Dirmhirn and Eaton

(1975). The old snow albedo value is 0.70 if no melting occurs during the time step and 0.50 if melting occurs. In the event of a snowfall, snow density is readjusted as the weighted average of the new snow density and the previous snow density, and snow albedo is refreshed back to 0.84. Snowmelt in the model occurs when the solution of the surface energy balance equation results in a temperature greater than 0°C or by heat conduction from the soil underneath the snowpack. The interception and unloading of snow on the canopy are modelled following Hedstrom and Pomeroy (1998). The snow amount intercepted during a snowfall event over a time step is obtained from the snow amount incident on the canopy during the time step, the initial intercepted snow amount and the interception capacity. The snow unloading rate is estimated from an empirical exponential function with a snow unloading coefficient value of  $0.1 \text{ d}^{-1}$  or  $1.157 \times 10^{-6} \text{ s}^{-1}$ .

In this study, five CRCM5 simulations covering the North American domain at 0.44° horizontal resolution are considered (Table 1). The first CRCM5 simulation spanning the 1958-2014 period is driven by ERA-40 (Uppala et al. 2005) for the 1958-1978 period and by ERA-Interim (Dee et al. 2011) for the 1979-2014 period, from the European Centre for Medium-range Weather Forecasting (ECMWF). This simulation will be referred to as CRCM5/ERA. The other four simulations are transient climate change simulations spanning the 1950-2100 period, driven by the second generation Canadian Earth System Model (CanESM2) (Arora et al. 2011) and the Max Planck Institute Earth System Model (MPI-ESM) (Giorgetta et al. 2013), for RCPs 4.5 and 8.5. The CanESM2-driven simulations will be referred to as CRCM5/Can4.5 and CRCM5/Can8.5, and similarly the MPI-ESM-driven simulations will be referred to as CRCM5/MPI4.5 and CRCM5/MPI8.5. The 1950-2005 period of both CRCM5/Can4.5 and CRCM5/Can8.5 are identical. Similarly, this is also the case for CRCM5/MPI4.5 and CRCM5/MPI8.5. Though the transient climate change simulations span the 1950-2100 period, only the current 1976-2005 period and the

future 2071-2100 period are considered for analysis in this article. It must be noted that for certain validations a slightly different current period is considered.

### 2.3 Methods and data

The performance errors, i.e. errors due to dynamics and physics of the regional model, are evaluated first by comparing the CRCM5/ERA simulated snow characteristics with available observations for the winter (DJF) and spring (MAM) seasons. Since 2-m air temperature and precipitation are two important variables indicating snow on the ground, they are also validated by comparing against the Climatic Research Unit (CRU) dataset. The CRU TS3.10 is a gridded dataset based on monthly observations at weather stations across the world's land areas (Mitchell and Jones 2005), which are interpolated on a  $0.5^{\circ}$  latitude/longitude global grid mesh, and is available for the 1961-2009 period.

CRCM5 simulated snow depth and SWE are validated against the Canadian Meteorological Centre (CMC) dataset. The CMC dataset provides daily snow depth and SWE (Brown et al. 2003) for the 1979-1997 period over North America at  $0.25^{\circ}$  resolution. A snow depth analysis scheme developed by Brasnett (1999) is used to interpolate the snow depth field with SWE estimated from empirical snow aging expressions. The scheme takes as input historical daily observations of snow depth (around 8000 per day) from the Canadian climate stations and from co-operating U.S stations.

Simulated snow cover and snow albedo are compared with the MOD10A1 product from the Moderate-Resolution Imaging Spectroradiometer (MODIS). The MOD10A1 uses the Terra satellite to provide daily global fractional snow cover and snow albedo data on a 500 m grid (Klein and Stroeve 2002). To determine fractional snow cover, MODIS uses an algorithm based on the normalized difference snow index (NDSI), which depends on the characteristic of snow being very reflective in

the visible bands and very absorptive in the near infrared bands (Riggs et al. 2006). Snow albedo is determined by a bi-directional reflectance distribution function (BRDF) model for snow (Stroeve et al. 2006), based on the discrete-ordinate radiative transfer (DISORT) model (Stamnes et al. 1998).

Simulated surface albedo is compared with the International Satellite Cloud Climatology Project (ISCCP) and the MODIS products, ISCCP-FD and MCD43C3, respectively. The ISCCP-FD (Zhang et al. 2004) is a product based on the ISCCP D1 (Rossow and Schiffer 1999) data collected from a suite of polar orbiting and geostationary satellites, and the NASA Goddard Institute for Space Studies (GISS) radiative transfer model (Hansen et al. 2002; Oinas et al. 2001). The MCD43C3 uses the BRDF (Wanner et al. 1995) to provide albedo values for cloud-free condition, in an 8 days composite and on a  $0.05^\circ$  longitude/latitude grid (Gao et al. 2005; Lucht et al. 2000; Schaaf et al. 2002).

The surface component of SAF in CRCM5 is also validated with MODIS data. As already discussed, following Qu and Hall (2007), the SAF strength is estimated as the amount of additional net shortwave radiation at the TOA as surface albedo decreases in association with an increase in surface air temperature, which yields the relation :

$$\frac{\partial Q_{TOA}^{net}}{\partial T_s} = -Q_{TOA}^{in} \frac{\partial \alpha_p}{\partial \alpha_s} \frac{\partial \alpha_s}{\partial T_s} = -Q_{TOA}^{in} \frac{\partial \alpha_p}{\partial \alpha_s} CAT, \quad (1)$$

Following Qu and Hall (2006), the variation in planetary albedo with surface albedo and CAT are computed as

$$\frac{\partial \alpha_p}{\partial \alpha_s} = T_a^{cr} - \varepsilon_2 c \ln(\tau + 1), \quad (2)$$

$$CAT = SCF + TDA, \quad (3)$$

where,

$$SCF = \frac{\Delta S_c}{\Delta T_s} (\overline{\alpha_{snow}} - \overline{\alpha_{land}}) \quad (4)$$

$$TDA = \bar{S}_c \frac{\Delta \alpha_{snow}}{\Delta T_s}. \quad (5)$$

In Eq. (1),  $Q_{TOA}^{net}$  and  $Q_{TOA}^{in}$  are respectively the net and incoming shortwave radiation at the TOA,  $T_s$  is the surface air temperature,  $\alpha_p$  is the planetary albedo, and  $\alpha_s$  is the surface albedo. In Eq. (2),  $T_a^{cr}$  is the effective clear-sky atmospheric transmissivity,  $\varepsilon_2$  is a linear coefficient,  $c$  is the cloud cover, and  $\tau$  is the cloud optical thickness.

In the seasonal cycle context, the deltas in Eqs. (4) and (5) represent the difference between May and April values of the representative variables, and the overbars represent the time mean computed over the two months for the 2001-2010 period. This period is chosen based on observation availability. In the climate change context, the deltas represent the difference between future (2071-2100) and current (1976-2005) MAM periods, and the overbars represent the time mean computed over the two MAM periods. The  $S_c$  represents the fractional snow cover,  $\alpha_{snow}$  represents snow albedo, which is defined when  $S_c$  is higher than 0.10, and  $\alpha_{land}$  represents the snow-free land albedo.

For the quantification of CAT in CRCM5,  $S_c$ ,  $\alpha_{snow}$ , and  $T_s$  are taken from the model output, in contrast with previous studies (Fletcher et al. 2012), where values of  $\alpha_{snow}$  are derived from surface albedo. For the quantification of observed CAT,  $S_c$  and  $\alpha_{snow}$  are taken from the MOD10A1 product and surface air temperature  $T_s$  is taken from the ERA-Interim reanalysis. The only unknown variable left is  $\alpha_{land}$ , which is derived from known variables. Assuming that surface albedo can be expressed by the following relation:

$$\alpha_s = S_c \alpha_{snow} + (1 - S_c) \alpha_{land}, \quad (6)$$

we can compute  $\alpha_{land}$  by rewriting Eq. (6) as

$$\alpha_{land} = \frac{\alpha_s - S_c \alpha_{snow}}{1 - S_c}. \quad (7)$$

The surface albedo  $\alpha_s$  is taken from the model output, as well as from the MCD43C3 product, for the white-sky case.

Projected changes to snow characteristics, i.e. snow cover, snow albedo and surface albedo, for the 2071-2100 period with respect to the 1976-2005 period, are assessed for the CRCM5/Can4.5, CRCM5/Can8.5, CRCM5/MPI4.5 and

CRCM5/MPI8.5 simulations. Prior to looking at projected changes, the boundary forcing errors, i.e. errors associated with the boundary forcing data, are assessed by comparing snow characteristics in CRCM5/Can4.5 and CRCM5/MPI4.5 with that of CRCM5/ERA for the current climate. This will help to identify regions where extra caution must be taken when interpreting projected changes.

The CAT, SCF, and TDA in the climate change context are assessed using Eqs. (3) to (5), for the four transient simulations as previously discussed. Comparison of the four simulations allows a better understanding of CAT sensitivity to driving data and RCPs. Finally, the five CRCM5 simulations are used to calculate the variation in planetary albedo with surface albedo and the SAF strength, in the seasonal cycle and the climate change contexts.

## 2.4 Results

### 2.4.1 Validation

In this section, validation of CRCM5 simulated 2-m temperature, precipitation, snow characteristics, and CAT are validated by comparing the CRCM5/ERA simulation with observations. This assessment is focussed on the biases in the snow dominant regions. Comparison of CRCM5/ERA 2-m air temperature with that from CRU (Figure 1a) suggests cold biases mainly over the western and central regions of the United States during winter. During spring, cold biases can be noted for the western mountainous regions, the northern Great Plains, and the boreal forests. Validation for the mountainous regions is often challenging, given the uncertainties in the observed data for these regions stemming from the lack of observations and insufficient resolution. There are also large biases in the Canadian Arctic Archipelago for both seasons. It should be noted however that the uncertainties in the observed air temperature are high for these regions due to few weather stations. For precipitation (Figure 1b), there is mostly a positive bias over the mountainous regions of the west

coast and some regions near the Great Lakes. In terms of temporal distribution, assessment of CRCM5 by Martynov et al. (2013) has shown that the model reproduces adequately the annual cycle of air temperature and precipitation over most parts of North America.

The comparison of snow depth and SWE with observations (Figures 2a and b) shows high overestimation over high latitudes such as the Canadian Arctic Archipelago and northeast regions of Canada. Simulated snow depth and SWE over the Canadian Arctic Archipelago (i.e. north of about 65°N) increase monotonically throughout the historical period. This monotonic increase, currently under investigation, is believed to be due to inadequate representation of snow transformation into glaciers. Note that observations also have uncertainties over these regions, as there are few weather stations over northern regions of Canada; station density decreases rapidly north of about 55°N (Brown et al. 2003). Large biases in snow depth and SWE can also be noted for the mountainous regions of western North America, similar to precipitation discussed previously. The CMC dataset contains a low elevation bias as well; reports of snow depth values in mountainous regions are less frequent, as snow course reports are done weekly, bi-weekly or monthly (Brown et al. 2003). A slight overestimation in snow depth and SWE can also be noted in MAM over the northern Great Plains. As can be seen from Figures 3a and b, the CRCM5/ERA simulation captures reasonably well the mean annual cycle of snow depth and SWE, averaged over a region covering 115°W–55°W, 40°N–65°N. Comparison of mean snow depth time series from CRCM5/ERA with that of CMC for the 1979–1997 period (Figure not shown) indicates a correlation of 0.50 for DJF and 0.56 for MAM, at 5% significance level. For SWE, a correlation of 0.40 is obtained for DJF, and a correlation of 0.73 at 1% significance level is obtained for MAM.

Results for snow cover and snow albedo in Figures 4 (a) and (b) show relatively good agreement between CRCM5/ERA and MODIS over the Great Plains

in winter and over high latitude areas in both seasons. However, a positive bias is noted for both variables over the boreal forests and the mountainous regions of western North America. This overestimation, particularly over the forested regions, can be explained by the uncertainties with the MODIS-based albedo values. Şorman et al. (2007) reported problems over complex terrain, as the MODIS algorithm considers snow as an isotropic surface over forests. Moreover, persistent cloud cover lasting many days over a region may prevent the satellite from detecting snow on the ground (Hall and Riggs 2007).

In Figures 5 (a) and (b), surface albedo from CRCM5/ERA simulation is validated against that from the ISCCP and the MODIS datasets. The two observation datasets, though generally similar, have slightly higher values in ISCCP compared to MODIS. Results show that CRCM5 is able to represent the spatial distribution of surface albedo with some overestimation over the Canadian Arctic Archipelago in winter, and over the northern Great Plains region in spring. The overestimation of surface albedo, snow depth, SWE, and the cold bias in 2-m air temperature over the northern Great Plains in spring point towards a late spring snowmelt in CRCM5. It appears that the model has difficulty in representing surface albedo in both vegetated and mountainous areas. A positive bias is noted over the boreal forests for both seasons, which can be partly explained by the inadequate representation of the snow unloading from the canopy (Bartlett and Verseghy 2015). Errors in surface albedo may also be related to the parameterizations of snow processes over complex terrain and satellite deficiencies in persistent cloud cover conditions, as discussed previously. Surface albedo annual cycles in Figure 3 (c) suggest an overestimation in CRCM5 compared to ISCCP, particularly during spring and summer, whereas Figure 3 (d) shows important overestimation in CRCM5 compared to MODIS during the winter and spring months. The time series of CRCM5 mean surface albedo (Figure not shown) reveal a correlation of 0.50 in DJF and 0.59 in MAM at 5% significance level when compared with ISCCP. Comparisons with MODIS indicate a correlation of 0.65 in DJF at 5% significance level and a correlation of 0.22 in MAM.

The CAT, SCF, and TDA in Figure 6 suggests important differences between CRCM5/ERA simulation and MODIS. Firstly, both CRCM5 and MODIS show a dominance of the SCF over the spring snowmelt and mountainous regions, and higher values of TDA over the higher latitudes. Although the two datasets seem to produce similar spatial patterns, regions with high SCF values in CRCM5 are slightly shifted southward compared to MODIS. This southward shift indicates that CRCM5 spring snowmelt occurs later compared to observations which is consistent with the snow depth, SWE, and surface albedo patterns seen over the northern Great Plains discussed previously. Moreover, the relatively simple snow cover parameterization, using a 0.10 m snow depth threshold, can partly explain the low values of simulated SCF over the high latitudes as snow cover remains constant and equal to 1 between April and May. Secondly, results show that the magnitude of the CRCM5 TDA term is considerably underestimated, while that of SCF is highly overestimated compared to observations. Averaged over the selected area shown in the inset of Figure 3 (a), the TDA component is estimated at  $-0.25 \text{ \%K}^{-1}$  in CRCM5 compared to the  $-0.70 \text{ \%K}^{-1}$  obtained with MODIS. The SCF component is  $-2.62 \text{ \%K}^{-1}$  in CRCM5 in contrast to  $-0.96 \text{ \%K}^{-1}$  when estimated with MODIS. This leads to an overestimation in the magnitude of the CRCM5 CAT that is mainly controlled by the SCF. The CAT is estimated at  $-2.87 \text{ \%K}^{-1}$  with CRCM5 and  $-1.66 \text{ \%K}^{-1}$  with MODIS. MODIS values for the three terms are in line with those from the Advanced Very High Resolution Radiometer satellite data seen in Fernandes et al. (2009); in both cases SCF and TDA over North America from satellite data show more or less similar strength with higher values for SCF, although the values of snow albedo are obtained differently. Overestimation in the magnitude of CAT due to SCF in the model is believed to have connections with the overestimation of snow albedo shown in the validation section, as Qu and Hall (2007) have shown that the SCF and the mean snow albedo are highly correlated in many GCMs.

#### 2.4.2 Projected changes

Before analyzing the projected changes to CRCM5 snow characteristics, the boundary forcing errors are assessed by comparing the CRCM5/Can4.5 and CRCM5/MPI4.5 simulations with the CRCM5/ERA simulation for the present period. As already mentioned, for the 1950-2005 period CRCM5/Can4.5 is the same as CRCM5/Can8.5 and CRCM5/MPI4.5 is the same as CRCM5/MPI8.5. For 2-m air temperature (Figure 1a), there are negative boundary forcing errors over the western United States in CRCM5/Can4.5. In CRCM5/MPI4.5 these negative errors extend over western Canada and Alaska in winter, and over the entire United States in spring. Positive boundary forcing errors can be noted over regions of northeast Canada in winter for both simulations. For precipitation (Figure 1b), positive errors are seen in CRCM5/Can4.5 over the west coast of Canada. In CRCM5/MPI4.5, there are negative errors over the west coast of Canada and positive errors covering the western United States in both seasons. The wet bias in precipitation over the southern areas is associated with the cold bias seen in 2-m air temperature of the CRCM5/MPI4.5 simulation, presumably through shortwave radiation reflection by clouds. These boundary forcing errors in air temperature and precipitation are consistent with those seen in Šeparović et al. (2013) where winter and summer seasons were assessed. It must be noted that errors for the regions receiving solid precipitation are very small for both GCM driven simulations.

Results for snow depth and SWE in Figures 2 (a) and (b) show that the CRCM5/ERA simulation and the GCM-driven simulations agree over most regions of the extratropics, with high positive boundary forcing errors over the Canadian Arctic Archipelago and the western coastal regions. Moreover, errors in snow depth and SWE are higher for CRCM5/MPI4.5 over eastern Canada and western United States. These positive errors are also captured in their annual cycle in Figures 3 (a) and (b). For snow cover (Figure 4a), results show positive boundary forcing errors over the United States in most cases, except for the MAM period of the CRCM5/Can4.5 simulation where negative boundary forcing errors are seen over Canada. For snow albedo (Figure 4b), the boundary forcing errors are almost

negligible, i.e. within  $\pm 3\%$ . As for surface albedo (Figures 5a and b), only small positive boundary forcing errors are noted over western mountainous regions of the United States, and over the northern Great Plains for the CRCM5/MPI4.5 simulation. These positive boundary forcing errors in surface albedo may have contributed to the negative boundary forcing errors in 2-m air temperature.

Results for projected changes to snow characteristics in Figure 7 show decreases in snow cover, snow albedo and surface albedo due to increases in air temperature associated with anthropogenic forcings. As expected, higher decreases in snow cover are seen for RCP 8.5 than for RCP 4.5. It is also important to note that CanESM2-driven simulations show higher snow cover loss compared to MPI-ESM-driven simulations, as 2-m air temperature increases are higher in CanESM2-driven simulations than in MPI-ESM-driven simulations. Snow albedo values show little decrease in projected climate change, with only a slightly higher signal for RCP 8.5 than for RCP 4.5 over eastern and western coastal areas. Decreases in surface albedo are high over the boreal forests, the northern Great Plains, and mountainous regions of western North America. As with snow cover, the decrease in surface albedo is also higher for RCP 8.5 than for RCP 4.5, and higher in CanESM2-driven simulations than in the MPI-ESM-driven simulations. This reflects well the dependence of surface albedo on snow cover. Compared to snow cover and surface albedo, projected changes to snow albedo shows less sensitivity to the RCPs and the lateral boundary forcings, thus indicating a very low dependence of snow albedo on air temperature, consistent with the parameterization used.

#### 2.4.3 CAT in the climate change context

Here, the CAT, SCF, and TDA are evaluated in the climate change context (Figure 8). Results for all four climate change simulations indicate a large SCF contribution compared to the TDA contribution to CAT. When compared with CAT in the seasonal cycle context, the magnitude of CAT simulated by CRCM5 in the climate

change context is much weaker. Comparison of CAT in the climate change context between RCP 4.5 and 8.5 shows very similar spatial distributions and magnitudes for both GCM driven simulations. Since the snow cover sensitivity to RCPs and lateral boundary forcings seen in the projected changes is not reflected in CAT, this result hints at a high dependence of CAT on snow albedo, which had low sensitivity to RCPs and lateral boundary forcings. The control of CAT by snow albedo was also reported in the study of Qu and Hall (2007).

The spatial distribution of TDA is further analyzed in Figure 9, which shows positive values over the Canadian Arctic Archipelago, for both seasonal cycle and climate change contexts. Generally, surface albedo decreases as surface air temperature increases, thus leading to a negative value of the feedback terms. In the Canadian Arctic Archipelago, surface albedo increases even if surface air temperature increases, and this is associated with higher frequency of snowfall and therefore albedo values as snowfall occurrence refreshes snow albedo back to its maximum value of 0.84. As reported by Langlois et al. (2014) and Wang et al. (2014), there seems to be a high sensitivity of the snow albedo parameterization to the snow albedo refreshment threshold.

#### 2.4.4 $\partial\alpha_p/\partial\alpha_s$ and SAF strength

In this section, the variation in planetary albedo with surface albedo  $\partial\alpha_p/\partial\alpha_s$  and SAF strength for the five simulations are analyzed (Figure 10). The  $\partial\alpha_p/\partial\alpha_s$ , i.e. the first factor of the formulation for SAF strength, is related to the attenuation effect of the atmosphere on the surface albedo anomalies. Simulations show similar spatial patterns of  $\partial\alpha_p/\partial\alpha_s$ , with higher values for the western United States, Mexico and some high latitude regions of Canada, and lower values for the eastern United States.  $\partial\alpha_p/\partial\alpha_s$  follows a similar spatial distribution to that of precipitation, which is reasonable since high precipitation is associated with cloudy sky and lower

transmissivity. In addition, the spatial distribution of  $\partial\alpha_p / \partial\alpha_s$  is also patchier in the seasonal cycle context as cloud variability is usually higher than that in the climate change context.

The SAF strength given by Eq. (1), for the five simulations, is shown in Figure 10. As with the CAT term, the magnitude of CRCM5 SAF strength in the seasonal cycle is high especially over the mountainous regions of western North America and the boreal forests, whereas in the climate change context the magnitude of SAF strength is much weaker. The high signals of  $\partial\alpha_p / \partial\alpha_s$  over the western United States and the high latitude regions of Canada lead to higher SAF strength in these areas. Aside from that,  $\partial\alpha_p / \partial\alpha_s$  does not exert a great impact on the spatial patterns of SAF strength; SAF strength preserves more or less the same spatial distribution as that of CAT.

## 2.5 Conclusions

The validation of CRCM5 simulated snow characteristics such as snow depth, SWE, snow cover, snow albedo, surface albedo, and CAT in the seasonal cycle context are presented in this article. Projected changes to these characteristics are also considered, along with CAT in the climate change context.

Snow characteristics in the CRCM5/ERA simulation are compared with CMC, MODIS and ISCCP observations. The CRCM5 and CMC comparison shows significant performance errors for snow depth and SWE over the Canadian Arctic Archipelago and the west coast mountains, which may be due to an inadequate representation of snow transformation into glaciers and complex snow processes over mountainous areas. However, the model is able to capture their spatial distributions and the annual cycles reasonably well over most parts of the midlatitude regions. Snow cover and snow albedo in CRCM5/ERA show good agreement with MODIS over high latitudes where snow is more intact, but a large positive bias for snow

albedo is noted over the boreal forests and the western mountains regions where snow is more subject to change and the parameterizations are more complex. The model shows skill in representing the main spatial distribution of surface albedo, but some overestimation over the boreal forests and the mountainous regions in Alaska were seen which indicates a rather late spring snowmelt compared to ISCCP and MODIS. It is also important to consider the presence of uncertainties among these observation-based datasets as values in ISCCP are higher than those in MODIS.

The CAT, SCF, and TDA are compared in the seasonal cycle with the CRCM5/ERA simulation and MODIS datasets. The simulated and observed CAT agree in spatial pattern; however the high values of the CRCM5 CAT are shifted southward compared to observations, which also suggests a late spring snowmelt in CRCM5/ERA. The magnitude of the CRCM5 TDA are underestimated, whereas that of the SCF is highly overestimated compared to MODIS. This leads to an overestimation in the magnitude of the CRCM5 CAT that is mainly controlled by the SCF. Furthermore, this positive bias in SCF over the midlatitude regions is believed to be related to the positive bias in snow albedo.

The CRCM5/Can4.5 and CRCM5/MPI4.5 simulations are compared with CRCM5/ERA simulation in order to assess boundary forcing errors. Results for snow depth and SWE show positive boundary forcing errors over the Canadian Arctic Archipelago and the west coast mountains. Very small boundary forcing errors are detected for snow cover and surface albedo over the United States and almost no boundary forcing error is detected for snow albedo. This indicates that the parameterizations of snow albedo have low sensitivity to the driving data.

Transient climate change simulations driven by CanESM2 and MPI-ESM for RCPs 4.5 and 8.5 indicate, as expected, loss in snow cover between future and present MAM periods along the southern limit of the snow-covered regions. The snow cover loss is higher for RCP 8.5 than for RCP 4.5, and higher in CanESM2-driven simulations than in MPI-ESM-driven simulations. Results for snow albedo values show very little decrease in projected climate change. Compared to snow

cover and surface albedo, snow albedo is less sensitive to the RCPs and driving data, thus more dependent on the parameterization in the model.

Very similar spatial distributions and magnitudes for CAT, SCF, and TDA are noted between RCPs 4.5 and 8.5 as well as for CanESM2- and MPI-ESM-driven simulations. Similar to the seasonal cycle, CAT in the climate change context is highly controlled by the SCF term. The SCF and snow albedo show similar properties as they both are highly sensitive to the parameterizations in the model. In addition, positive values of TDA over high latitudes are associated with an increase of snowfall occurrence in the seasonal cycle and in the climate change context, as snowfall refreshes snow albedo back to its maximum value.

Values of CAT, SCF, and TDA may depend upon many factors such as the model formulation, the quality of validation datasets, the parameterization of snow characteristics and the calculation method that are used. Comparison of observed and modelled SAF presented in this paper shows important differences, highlighting the need for an improved representation of snow albedo parameterization in the model.

### Acknowledgements

This research was undertaken within the framework of the Canadian Network for Regional Climate and Weather Processes (CNRCWP), funded by the Natural Sciences and Engineering Research Council's (NSERC) Climate Change and Atmospheric Research (CCAR) program.



## **FIGURES**

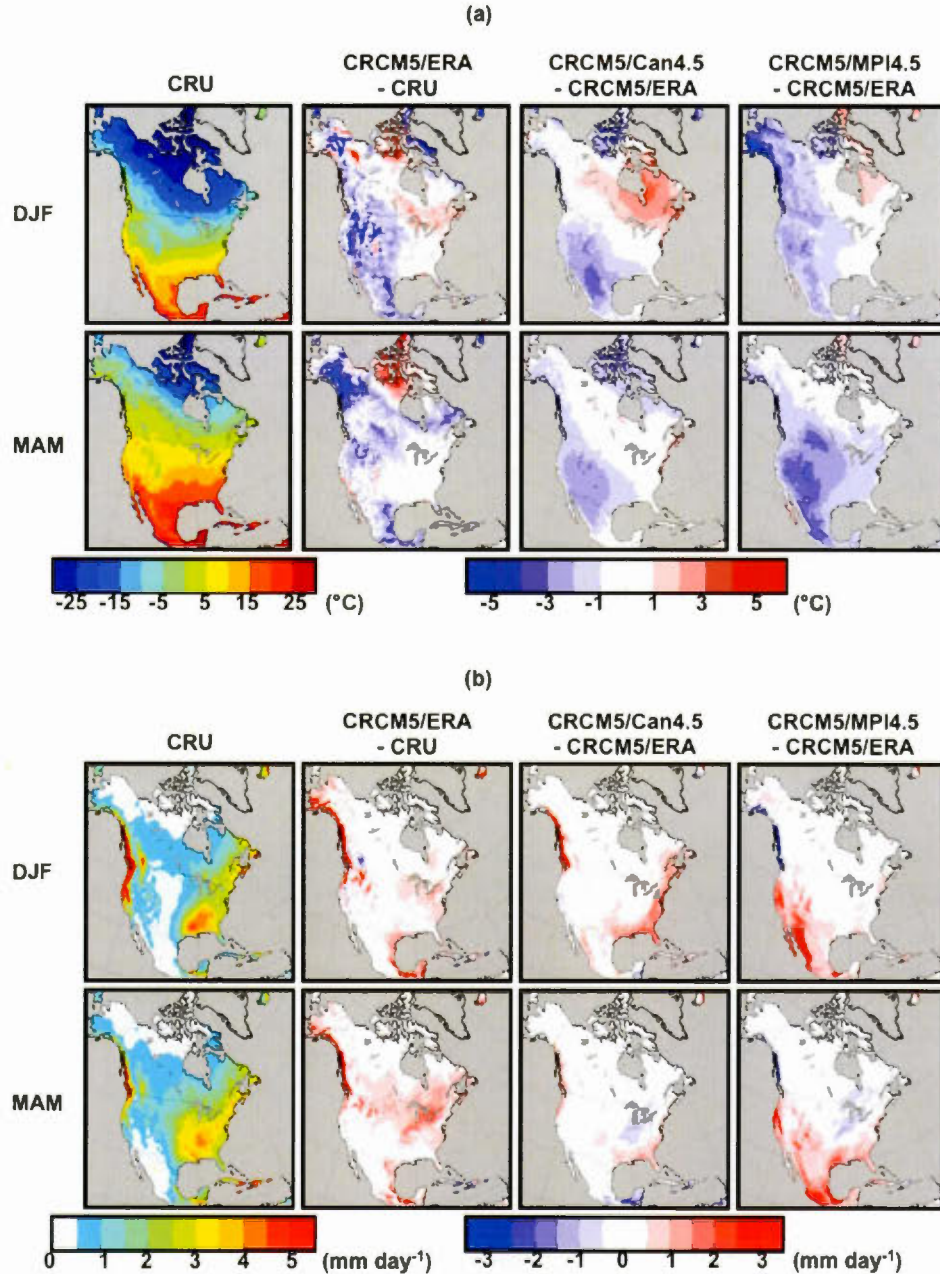


Figure 2.1: (a) Mean 2-m air temperature from CRU (first column), difference between CRCM5 driven by ERA-40/ERA-Interim and CRU (second column), difference between CRCM5 driven by CanESM2 and CRCM5 driven by ERA-40/ERA-Interim (third column), and difference between CRCM5 driven by MPI-ESM and CRCM5 driven by ERA-40/ERA-Interim (fourth column), for the 1976-2009 period. (b) Same as in (a) but for precipitation rate for the 1998-2008 period.

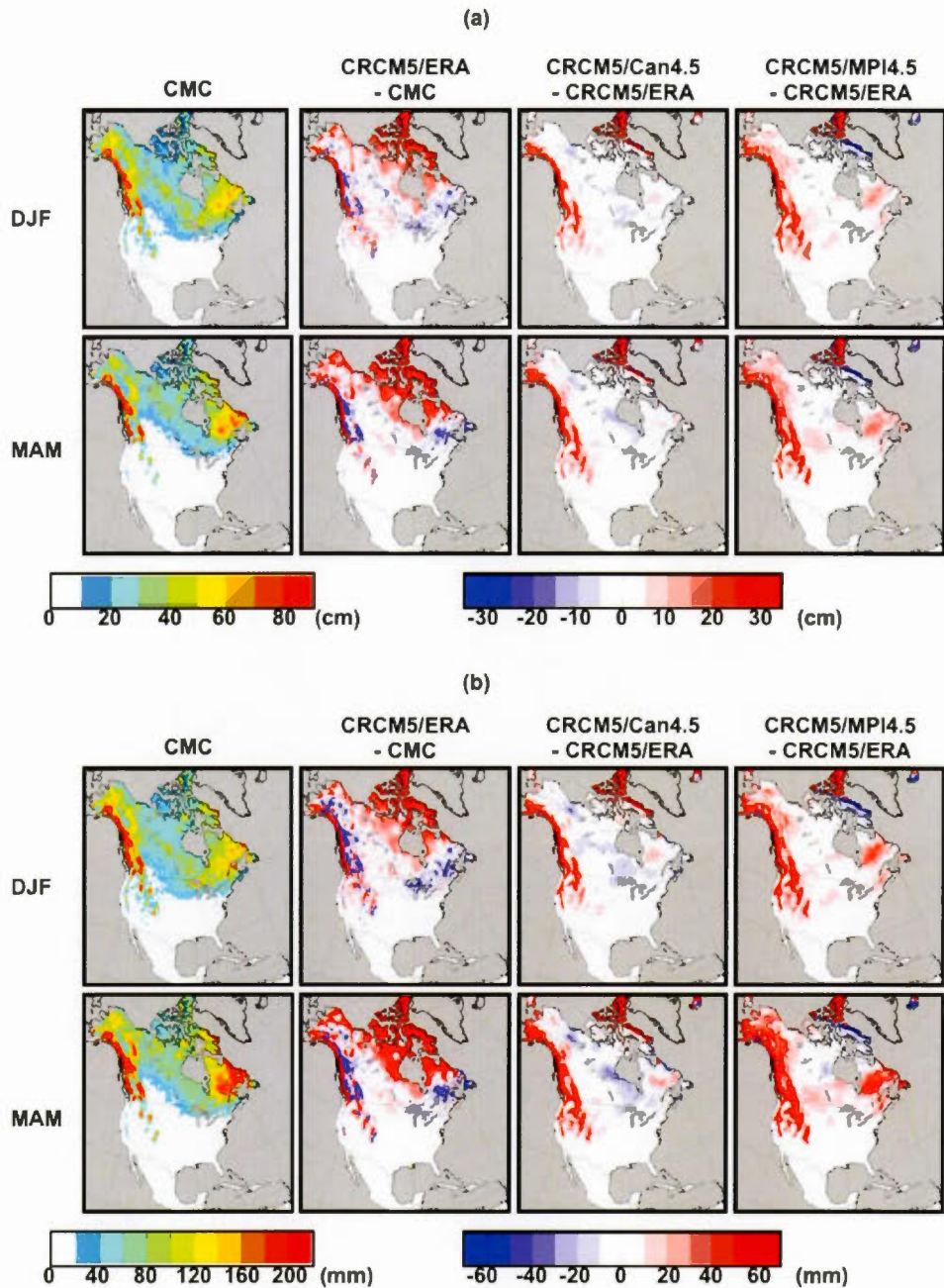


Figure 2.2: (a) Mean snow depth from CMC (first column), difference between CRCM5 driven by ERA-40/ERA-Interim and CMC (second column), difference between CRCM5 driven by CanESM2 and CRCM5 driven by ERA-40/ERA-Interim (third column), and difference between CRCM5 driven by MPI-ESM and CRCM5 driven by ERA-40/ERA-Interim (fourth column), for the 1979-1997 period. (b) Same as in (a) but for SWE.

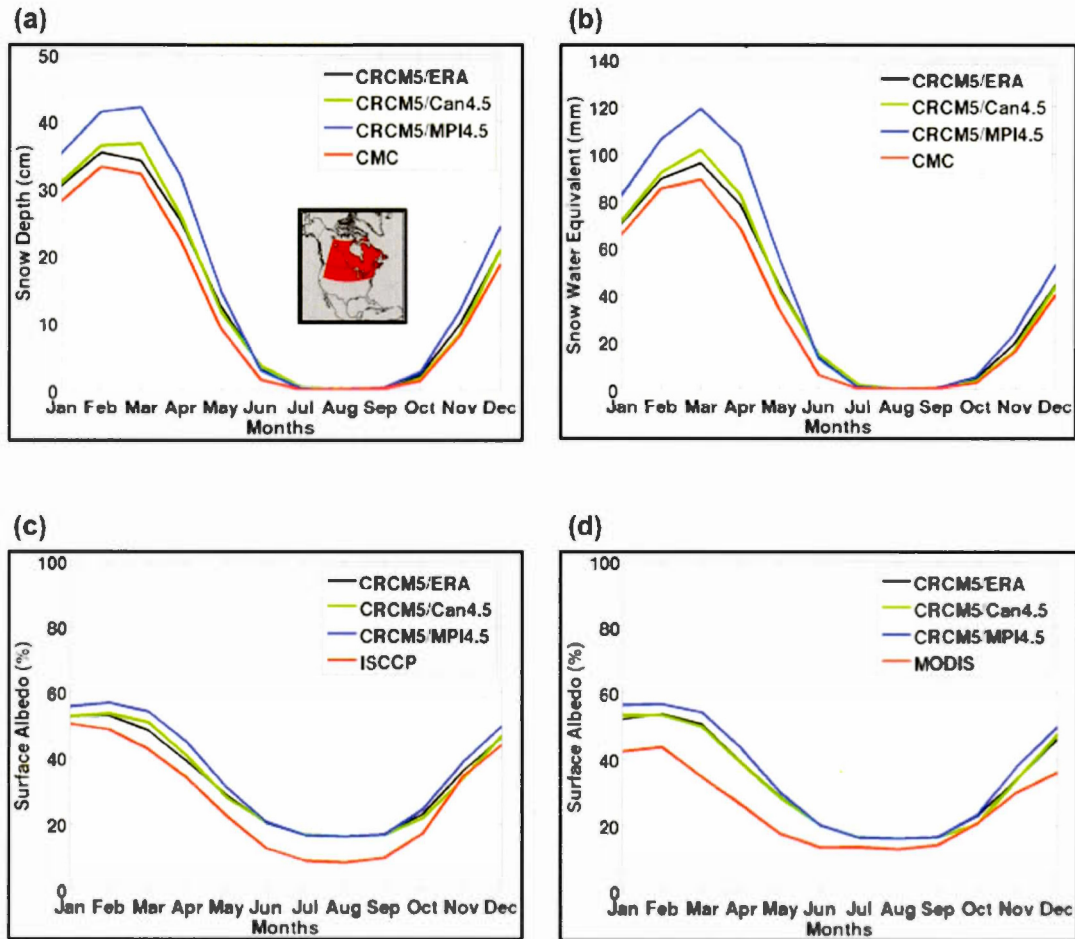


Figure 2.3: Model simulated and observed annual cycle of (a) snow depth, (b) SWE, and (c,d) surface albedo for a part of the midlatitude regions ( $115^{\circ}\text{W}$ - $55^{\circ}\text{W}$ ,  $40^{\circ}\text{N}$ - $65^{\circ}\text{N}$ ). (a) and (b) correspond to the 1979-1997 period, (c) and (d) correspond to the 1984-2000 and 2001-2010 periods, respectively. CRCM5 driven by ERA-40/ERA-Interim is in a black line, CRCM5 driven by CanESM2 is in a green line, CRCM5 driven by MPI-ESM is in a blue line, and observation is in a red line.

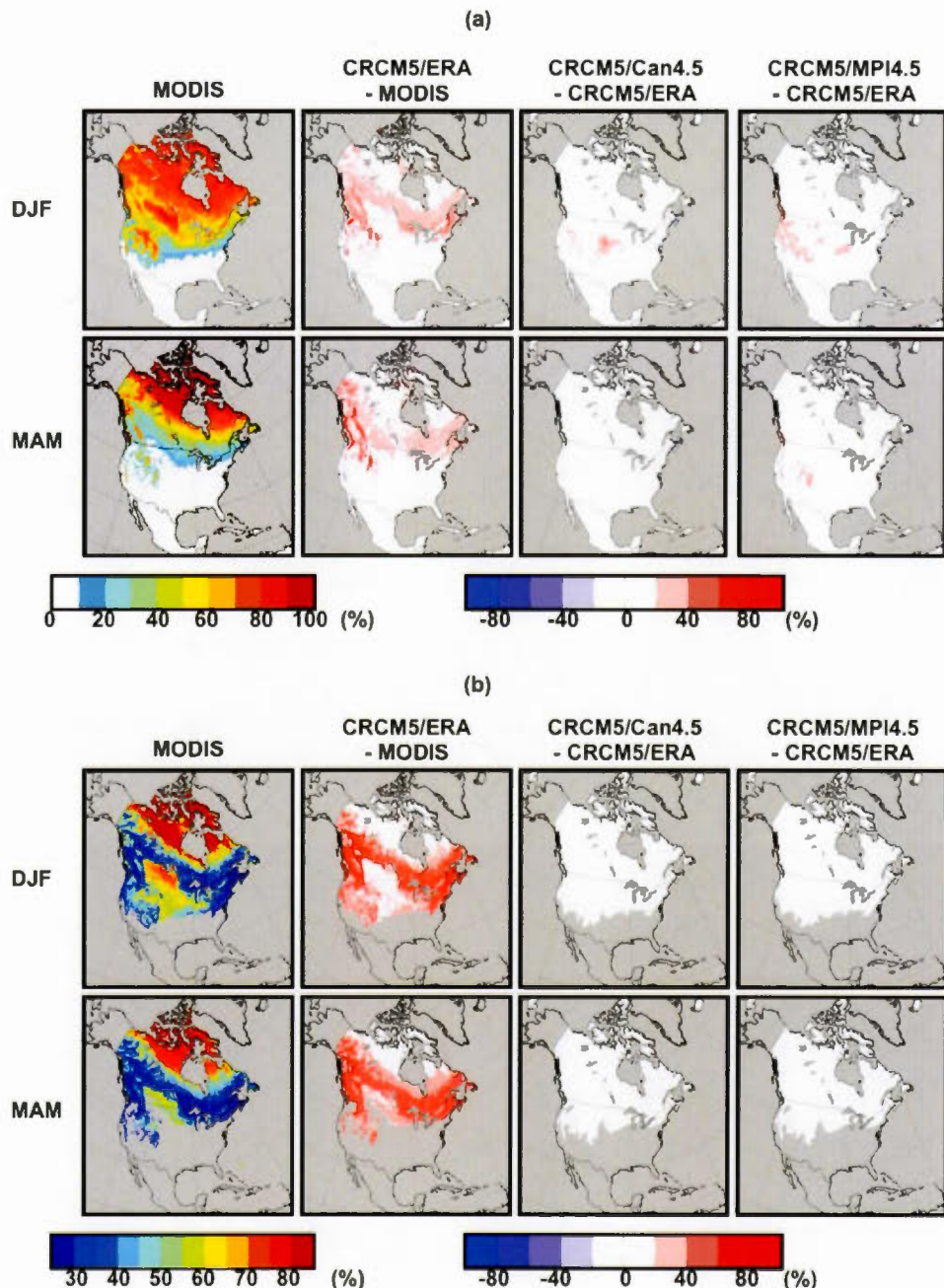


Figure 2.4: (a) Mean snow cover from MODIS (first column), difference between CRCM5 driven by ERA-40/ERA-Interim and MODIS (second column), difference between CRCM5 driven by CanESM2 and CRCM5 driven by ERA-40/ERA-Interim (third column), and difference between CRCM5 driven by MPI-ESM and CRCM5 driven by ERA-40/ERA-Interim (fourth column), for the 2001-2010 period. (b) Same as in (a) but for snow albedo.

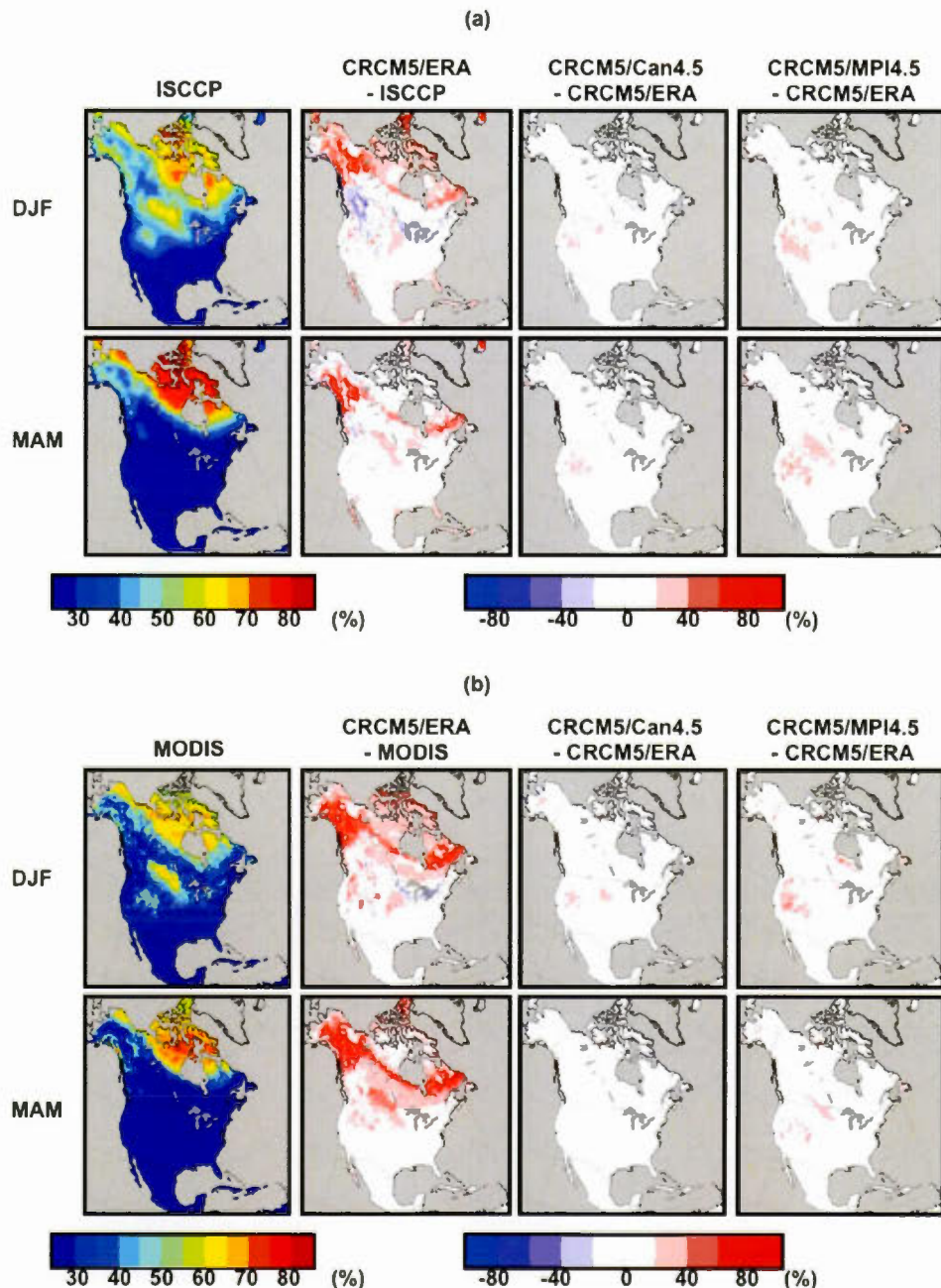


Figure 2.5: Mean surface albedo from (a) ISCCP (first column), difference between CRCM5 driven by ERA-40/ERA-Interim and ISCCP (second column), difference between CRCM5 driven by CanESM2 and CRCM5 driven by ERA-40/ERA-Interim (third column), and difference between CRCM5 driven by MPI-ESM and CRCM5 driven by ERA-40/ERA-Interim (fourth column), for the 1984-2000 period. (b) Same as in (a) but for MODIS for the 2001-2010 period.

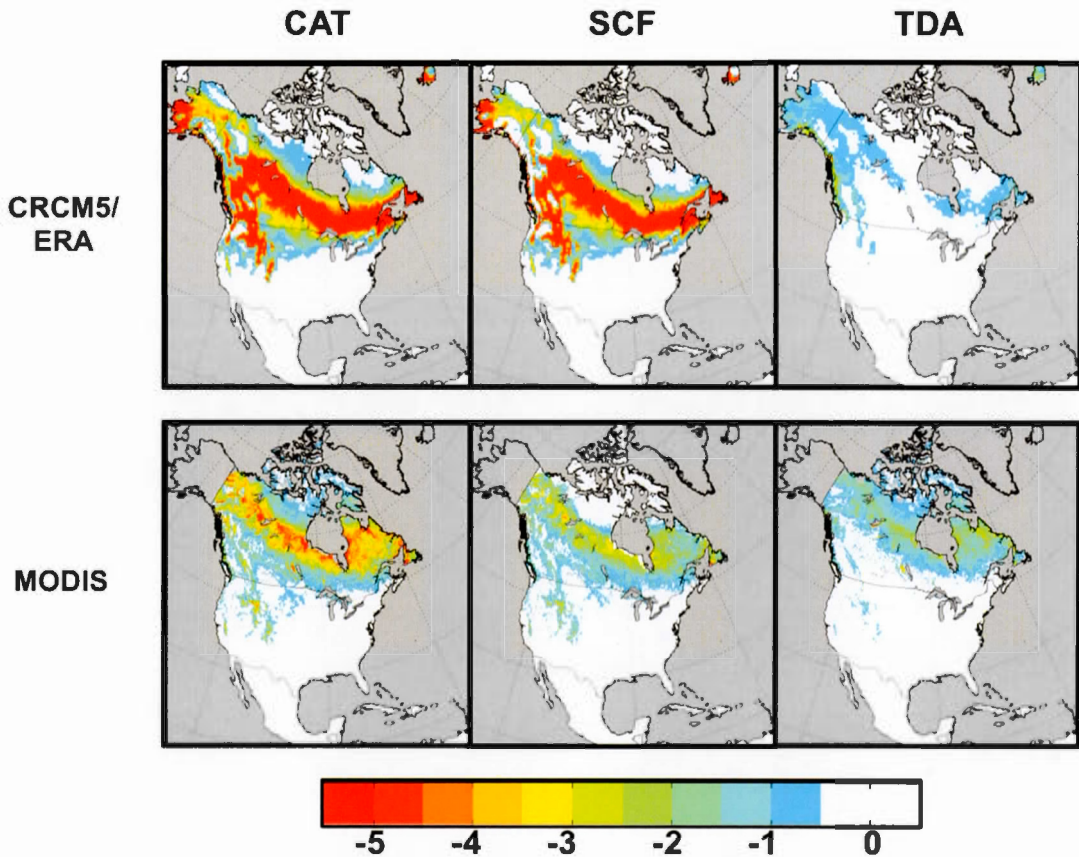


Figure 2.6: Change in surface albedo associated with surface air temperature change (first column;  $\% \text{ K}^{-1}$ ), snow cover feedback (second column;  $\% \text{ K}^{-1}$ ), and air temperature dependence of snow albedo (third column;  $\% \text{ K}^{-1}$ ) in the seasonal cycle context between May and April of the 2001-2010 period, from CRCM5 driven by ERA-40/ERA-Interim (first row) and MODIS (second row).

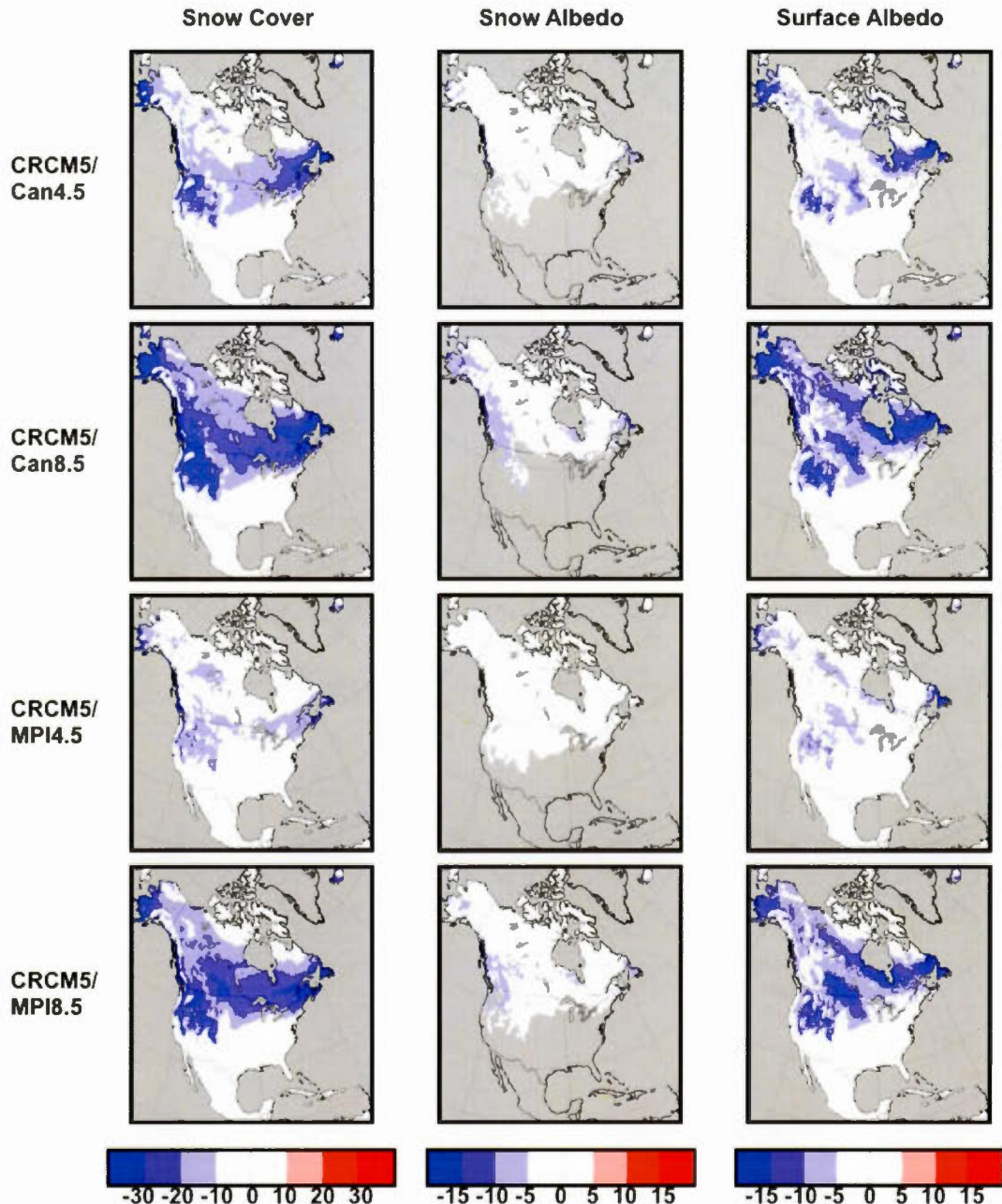


Figure 2.7: Projected changes to snow cover (first column; %), snow albedo (second column; %), and surface albedo (third column; %), for the 2071-2100 MAM period with respect to the 1976-2005 MAM period. CRCM5 driven by CanESM2 RCP 4.5 (first row), CRCM5 driven by CanESM2 RCP 8.5 (second row), CRCM5 driven by MPI-ESM RCP 4.5 (third row), and CRCM5 driven by MPI RCP 8.5 (fourth row). Grid points with no snow are masked in grey in the middle column.

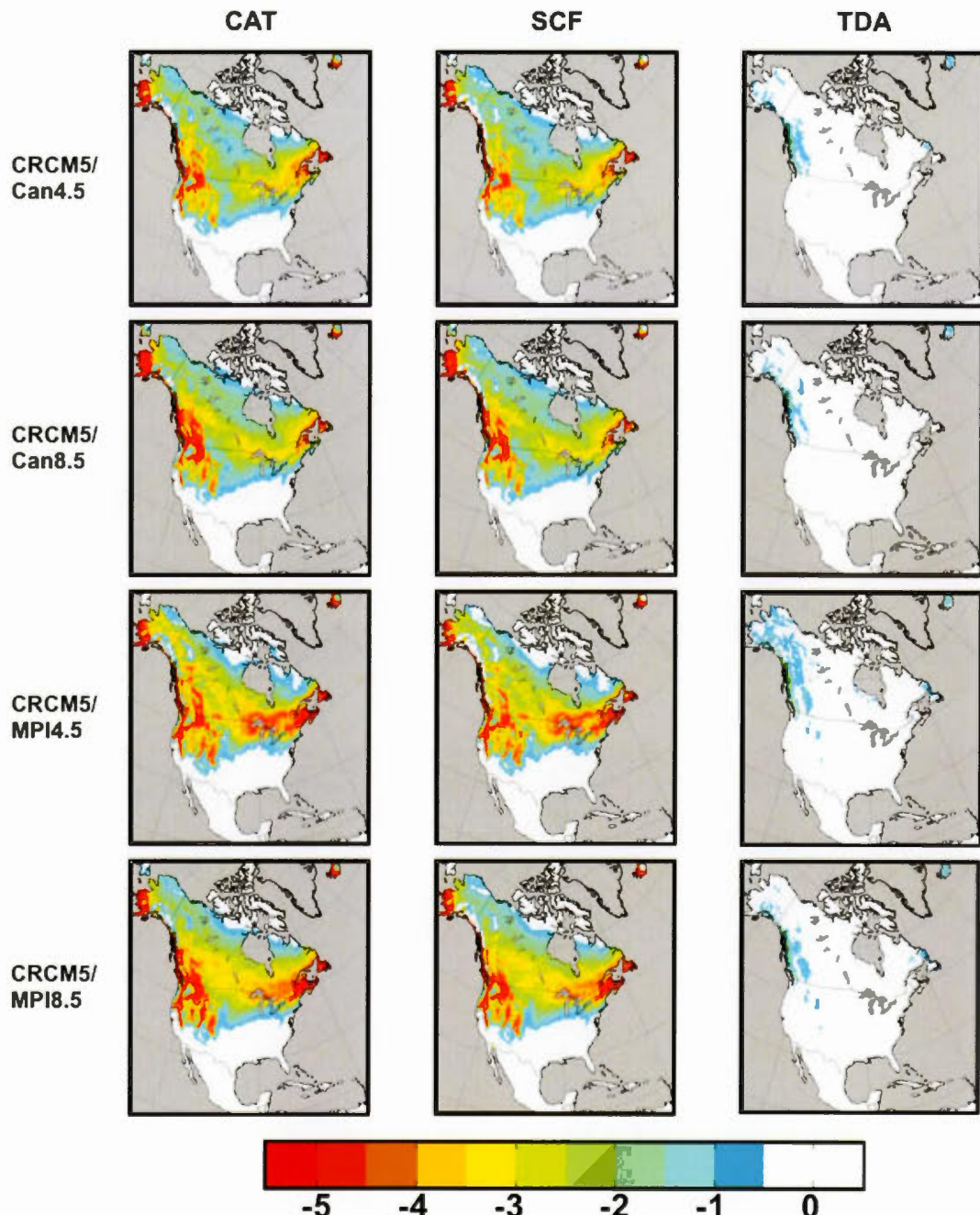


Figure 2.8: Change in surface albedo associated with air temperature change (first column;  $\% \text{ K}^{-1}$ ), snow cover feedback (second column;  $\% \text{ K}^{-1}$ ), and air temperature dependence of snow albedo (third column;  $\% \text{ K}^{-1}$ ) in the climate change context between the 2071-2100 MAM period and the 1976-2005 MAM period.

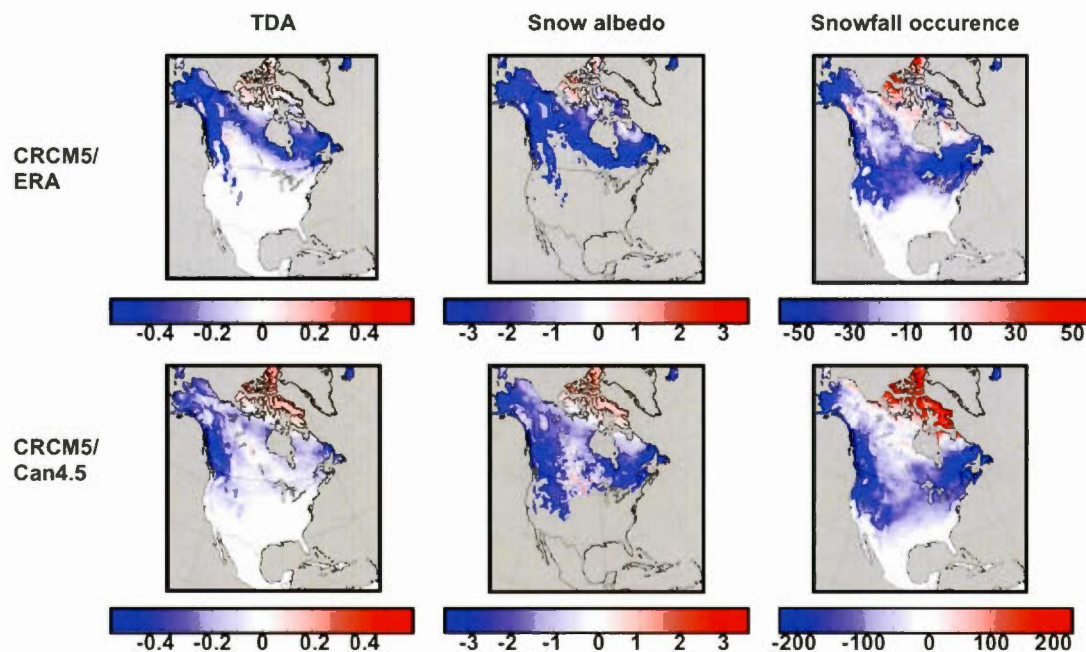


Figure 2.9: Air temperature dependence of snow albedo (first column;  $\% \text{ K}^{-1}$ ), snow albedo changes (second column; %), and snowfall occurrence changes (third column; days) in the seasonal cycle context (first row) and in the climate change context (second row), based on CRCM5 driven by ERA-40/ERA-Interim and CRCM5 driven by CanESM2 RCP 4.5.

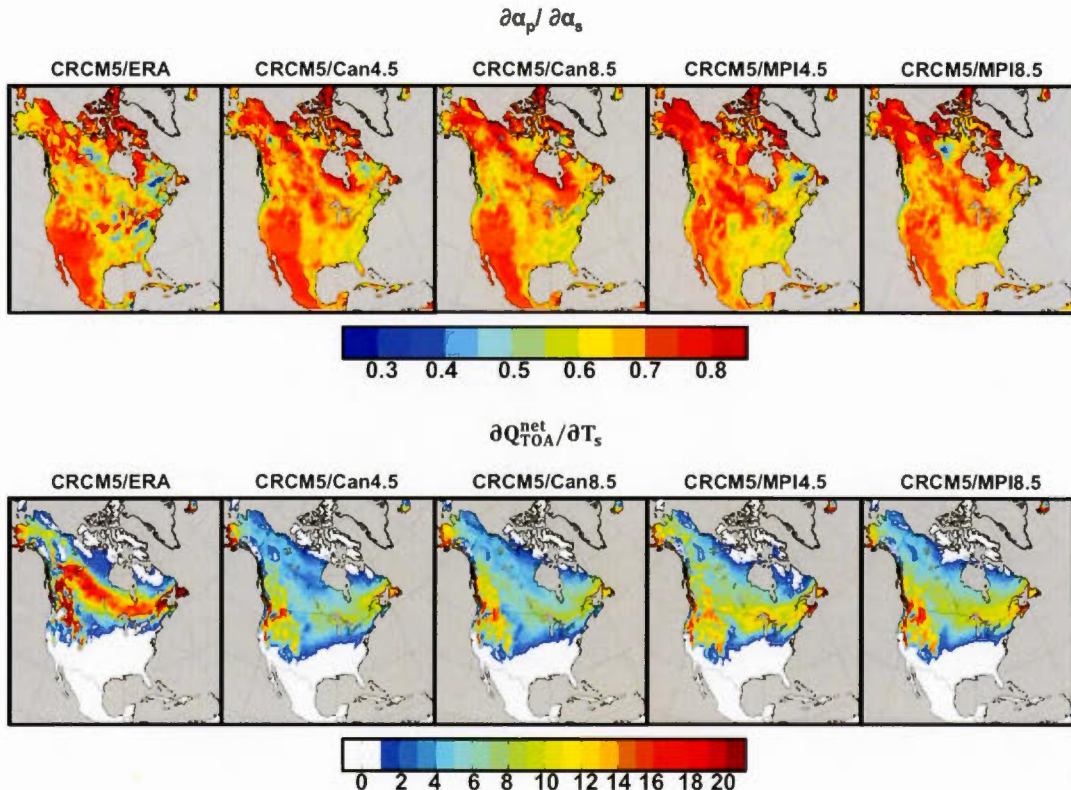


Figure 2.10: Variation in planetary albedo with surface albedo (top) and SAF strength (bottom;  $\text{W m}^{-2} \text{K}^{-1}$ ) in the seasonal cycle context (first column) and in the climate change context (second, third, fourth and fifth column), based on CRCM5 driven by ERA-40/ERA-Interim, CRCM5 driven by CanESM2 for RCP 4.5 and 8.5, and CRCM5 driven by MPI-ESM for RCP 4.5 and 8.5.



## TABLEAUX

Tableau 1.1 : The five CRCM5 simulations used in this study (first column), the corresponding simulation periods (second column), driving data (third column), and analysis periods (fourth column).

Simulations	Simulation periods	Driving data	Analysis periods
CRCM5/ERA	1958-2014	ERA-40 for 1958-1978 ERA-Interim for 1979-2014	1976-2010
CRCM5/Can4.5	1950-2100	CanESM2 (RCP 4.5)	1976-2005 2071-2100
CRCM5/Can8.5	1950-2100	CanESM2 (RCP 8.5)	1976-2005 2071-2100
CRCM5/MPI4.5	1950-2100	MPI-ESM (RCP 4.5)	1976-2005 2071-2100
CRCM5/MPI8.5	1950-2100	MPI-ESM (RCP 8.5)	1976-2005 2071-2100





## CHAPITRE III

### DISCUSSION DES RÉSULTATS ET CONCLUSIONS

Dans cette étude, une validation est effectuée pour les caractéristiques de la neige et le CAT en Amérique du Nord tel que simulé par le MRCC5. Les erreurs de performance sont évaluées en comparant la simulation du MRCC5 piloté par les réanalyses ERA-40/ERA-Interim avec les observations disponibles. La validation montre que le MRCC5 capte bien la distribution spatiale de la profondeur et l'équivalent en eau de la neige dans la plupart des régions des latitudes moyennes, par contre il y a des incertitudes significatives dans l'archipel arctique canadien et sur les régions montagneuses de l'Ouest. Ces incertitudes sont possiblement reliées à une représentation inadéquate de la transformation de la neige en glacier et de la complexité des processus physiques de la neige sur les régions montagneuses. Un manque de stations météorologiques dans les hautes latitudes peut également contribuer à expliquer les incertitudes des données observées. Le MRCC5 simule relativement bien le cycle annuel de la profondeur de la neige et de l'équivalent en eau de la neige. La couverture neigeuse et l'albédo de la neige simulés montrent une compatibilité avec les observations seulement dans les hautes latitudes où la neige est plus intacte. On observe un grand biais positif pour l'albédo de la neige dans les

forêts boréales et les montagnes de l'Ouest où la neige est plus sujette au changement et où le paramétrage est plus complexe. Le modèle est en mesure de représenter la distribution spatiale de l'albédo de la surface avec une surestimation dans les forêts boréales et les régions montagneuses en Alaska, indiquant une fonte de la neige printanière tardive comparée aux observations. Le cycle annuel pour l'albédo de la surface montre qu'il y a une surestimation qui est plus grande lorsque comparé avec MODIS que lorsque comparé avec ISCCP, ce qui indique la présence des certitudes parmi les données d'observations.

Le CAT, la SCF et la TDA sont quantifiés dans le cycle saisonnier avec la simulation du MRCC5 pilotée par ERA-40/ERA-Interim et les données de MODIS afin de réaliser une validation. Le CAT simulé et le CAT observé s'entendent sur la répartition spatiale, par contre la région couverte par le CAT dans le MRCC5 est décalé vers le sud comparé aux observations, ce qui suggère encore une fois une fonte de la neige printanière tardive dans le modèle. L'amplitude de la TDA dans le MRCC5 est plutôt sous-estimée alors que l'amplitude de la SCF est grandement surestimée comparé aux observations. Ceci mène donc à une surestimation du CAT du MRCC5 qui est principalement contrôlée par la SCF. Le biais positif de la SCF dans latitudes moyennes semble être relié au biais positif de l'albédo de la neige montré dans la validation. Ce lien a également été établie dans les études de Qu et Hall (2007), montrant une grande corrélation entre la SCF et l'albédo de la neige dans les MCGs.

Les simulations pilotées par CanESM2 et MPI-ESM sont comparées avec la simulation pilotée par ERA-40/ERA-Interim pour évaluer les erreurs de condition aux frontières. Les résultats pour la profondeur de la neige et l'équivalent en eau de la neige montrent des grandes erreurs de condition aux frontières sur l'archipel arctique canadien et les montagnes de l'Ouest. Ces erreurs de condition aux frontières sont également plus grandes dans la simulation pilotée par MPI-ESM que dans la simulation pilotée par CanESM2. Il n'y a presque pas d'erreur de condition aux frontières pour la couverture neigeuse et l'albédo de la neige, ce qui indique qu'ils sont très sensibles à leurs paramétrages dans le modèle régional du climat. Pour l'albédo de la surface, on observe seulement que de faibles erreurs de condition aux frontières pour les régions montagneuses à l'ouest des États-Unis.

Les simulations de changement climatique transitoire pilotée par CanESM2 et MPI-ESM sont utilisées pour évaluer les changements projetés des caractéristiques de la neige pour les RCPs 4.5 et 8.5. Les résultats indiquent une diminution de la couverture neigeuse à la limite sud des régions couvertes de neige. Cette diminution est plus grande pour le RCP 8.5 que pour le RCP 4.5, et plus grande dans la simulation pilotée par CanESM2 que dans la simulation pilotée par MPI-ESM. Les résultats pour les valeurs d'albédo de la neige montrent de faible diminution dans le changement projeté. Comparé à la couverture neigeuse et à l'albédo de la surface, l'albédo de la neige est moins sensible aux RCPs et aux données de pilotage, donc plus sensible aux paramétrages dans le modèle.

Le CAT, la SCF et la TDA sont évalués dans le contexte du changement climatique. Les distributions spatiales et les amplitudes sont très similaires entre les simulations pilotées par CanESM2 et MPI-ESM, et même entre les RCPs 4.5 et 8.5. Ceci montre que les termes sont très sensibles aux paramétrages dans le modèle, semblable aux changements projetés de l'albédo de la neige. De plus, les valeurs positives de la TDA dans les hautes latitudes sont associées à une augmentation des chutes de neige dans le cycle saisonnier et dans le changement climatique, la chute de neige renouvelle l'albédo de la neige à sa valeur maximale.

Les valeurs du CAT, de la SCF et de la TDA peuvent dépendre de plusieurs facteurs tels que la formulation du modèle, la qualité des données d'observations, le type de paramétrage des caractéristiques de la neige et la méthode de calcul utilisés. La comparaison de la rétroaction de l'albédo de la neige observée et modélisée dans cette étude montre des différences importantes, soulignant le besoin d'une meilleure représentation dans le paramétrage de l'albédo de la neige dans le modèle.





## RÉFÉRENCES

- Aguado E (1985) Radiation balances of melting snow covers at an open site in the central Sierra Nevada, California. *Water Resources Research*, 21(11), 1649-1654.
- Arora VK, Scinocca JF, Boer GJ, Christian JR, Denman KL, Flato GM, Kharin VV, Lee WG, Merryfield WJ (2011) Carbon emission limits required to satisfy future representative concentration pathways of greenhouse gases. *Geophysical Research Letters*, 38(5), L05805.
- Barnes WL, Pagano TS, Salomonson VV (1998) Prelaunch characteristics of the moderate resolution imaging spectroradiometer (MODIS) on EOS-AM1. *Geoscience and Remote Sensing, IEEE Transactions on*, 36(4), 1088-1100.
- Bartlett PA, Verseghy DL (2015) Modified treatment of intercepted snow improves the simulated forest albedo in the Canadian Land Surface Scheme. *Hydrological Processes*, 29(14), 3208-3226.
- Bélair S, Mailhot J, Girard C, Vaillancourt P (2005) Boundary layer and shallow cumulus clouds in a medium-range forecast of a large-scale weather system. *Monthly weather review*, 133(7), 1938-1960.
- Benoit R, Côté J, Mailhot J (1989) Inclusion of a TKE boundary layer parameterization in the Canadian regional finite-element model. *Monthly weather review*, 117(8), 1726-1750.
- Brasnett B (1999) A global analysis of snow depth for numerical weather prediction. *Journal of Applied Meteorology*, 38(6), 726-740.

- Brown RD, Brasnett B, Robinson D (2003) Gridded North American monthly snow depth and snow water equivalent for GCM evaluation. *Atmosphere-Ocean*, 41(1), 1-14.
- Côté J, Gravel S, Méthot A, Patoine A, Roch M, Staniforth A (1998) The operational CMC-MRB global environmental multiscale (GEM) model. Part I: Design considerations and formulation. *Monthly Weather Review*, 126(6), 1373-1395.
- Dee DP, Uppala SM, Simmons AJ et al (2011) The ERA-Interim reanalysis: Configuration and performance of the data assimilation system. *Quarterly Journal of the Royal Meteorological Society*, 137(656), 553-597.
- Delage Y (1997) Parameterising sub-grid scale vertical transport in atmospheric models under statically stable conditions. *Boundary-Layer Meteorology*, 82(1), 23-48.
- Delage Y, Girard C (1992) Stability functions correct at the free convection limit and consistent for both the surface and Ekman layers. *Boundary-Layer Meteorology*, 58(1-2), 19-31.
- Dirmhirn I, Eaton FD (1975) Some characteristics of the albedo of snow. *Journal of Applied Meteorology*, 14(3), 375-379.
- Essery R (2013) Large-scale simulations of snow albedo masking by forests. *Geophysical Research Letters*, 40(20), 5521-5525.
- Fernandes R, Zhao H, Wang X, Key J, Qu X, Hall A (2009). Controls on northern hemisphere snow albedo feedback quantified using satellite Earth observations. *Geophysical Research Letters*, 36(21), L21702.
- Fletcher CG, Zhao H, Kushner P, Fernandes R (2012) Using models and satellite observations to evaluate the strength of snow albedo feedback. *Journal of Geophysical Research : Atmospheres*, 117(D1), D11117.
- Gao F, Schaaf CB, Strahler AH, Roesch A, Lucht W, Dickinson R (2005) MODIS bidirectional reflectance distribution function and albedo Climate Modeling

- Grid products and the variability of albedo for major global vegetation types. *Journal of Geophysical Research: Atmospheres* (1984–2012), 110(D1), D01104.
- Giorgetta MA, Jungclaus J, Reick CH, Legutke S, Bader J, Böttinger M et al (2013) Climate and carbon cycle changes from 1850 to 2100 in MPI-ESM simulations for the Coupled Model Intercomparison Project phase 5. *Journal of Advances in Modeling Earth Systems*, 5(3), 572-597.
- Gold LW (1958) Changes in shallow snow cover subject to a temperate climate. *Journal of Glaciology*, 3, 218-222.
- Hall A (2004) The role of surface albedo feedback in climate. *Journal of Climate*, 17(7), 1550-1568.
- Hall A, Qu X (2006) Using the current seasonal cycle to constrain snow albedo feedback in future climate change. *Geophysical Research Letters*, 33(3), L03502.
- Hall A, Qu X, Neelin JD (2008) Improving predictions of summer climate change in the United States. *Geophysical Research Letters*, 35(1), L01702.
- Hall DK, Riggs GA (2007) Accuracy assessment of the MODIS snow products. *Hydrological Processes*, 21(12), 1534-1547.
- Hansen J, Sato M, Nazarenko L, Ruedy R, Lacis A, Koch D et al (2002). Climate forcings in Goddard Institute for Space Studies SI2000 simulations. *Journal of Geophysical Research: Atmospheres* (1984–2012), 107(D18), 4347.
- Hedstrom NR, Pomeroy JW (2002). Measurements and modelling of snow interception in the boreal forest. *Hydrological Processes*, 12(1011), 1611-1625.
- Kain JS, Fritsch JM (1990) A one-dimensional entraining/detraining plume model and its application in convective parameterization. *Journal of the Atmospheric Sciences*, 47(23), 2784-2802.

- Klein AG, Stroeve J (2002) Development and validation of a snow albedo algorithm for the MODIS instrument. *Annals of Glaciology*, 34(1), 45-52.
- Kuo HL (1965) On formation and intensification of tropical cyclones through latent heat release by cumulus convection. *Journal of the Atmospheric Sciences*, 22(1), 40-63.
- Langlois A, Bergeron J, Brown R, Royer A, Harvey R, Roy A et al (2014) Evaluation of CLASS 2.7 and 3.5 simulations of snow properties from the Canadian Regional Climate Model (CRCM4) over Québec, Canada. *Journal of Hydrometeorology*, 15(4), 1325-1343.
- Laprise R (1992) The Euler equations of motion with hydrostatic pressure as an independent variable. *Monthly weather review*, 120(1), 197-207.
- Letcher TW, Minder JR (2015) Characterization of the simulated regional snow albedo feedback using a regional climate model over complex terrain. *Journal of Climate*, 28(19), 7576-7595.
- Li J, Barker HW (2005) A radiation algorithm with correlated-k distribution. Part I: Local thermal equilibrium. *Journal of the atmospheric sciences*, 62(2), 286-309.
- Longley RW (1960) Snow depth and snow density at resolute, Northwest Territories. *Journal of Glaciology*, 3, 733-738.
- Loranty MM, Berner LT, Goetz SJ, Jin Y, Randerson JT (2014) Vegetation controls on northern high latitude snow-albedo feedback: observations and CMIP5 model simulations. *Global change biology*, 20(2), 594-606.
- Lucht W, Schaaf CB, Strahler AH (2000) An algorithm for the retrieval of albedo from space using semiempirical BRDF models. *IEEE Transactions on Geoscience and Remote Sensing*, 38(2), 977-998.
- Martynov A, Laprise R, Sushama L, Winger K, Šeparović L, Dugas B (2013) Reanalysis-driven climate simulation over CORDEX North America domain

- using the Canadian Regional Climate Model, version 5: model performance evaluation. *Climate Dynamics*, 41(11-12), 2973-3005.
- Masson V, Champeaux J-L, Chauvin F, Meriguet Ch, Lacaze R (2003) A global database of land surface parameters at 1-km resolution in meteorological and climate models. *Journal of Climate*, 16, 1261-1282.
- McFarlane NA (1987) The effect of orographically excited gravity wave drag on the general circulation of the lower stratosphere and troposphere. *Journal of the atmospheric sciences*, 44(14), 1775-1800.
- Mironov D, Heist E, Kourzeneva E, Ritter B, Schneider N, Terzhevik A (2010) Implementation of the lake parameterisation scheme FLake into the numerical weather prediction model COSMO. *Boreal environment research*, 15(2), 218-230.
- Mitchell TD, Jones PD (2005) An improved method of constructing a database of monthly climate observations and associated high-resolution grids. *International journal of climatology*, 25(6), 693-712.
- Oinas V, Lacis AA, Rind D, Shindell DT, Hansen JE (2001) Radiative cooling by stratospheric water vapor: Big differences in GCM results. *Geophysical research letters*, 28(14), 2791-2794.
- Qu X, Hall A (2006) Assessing snow albedo feedback in simulated climate change. *Journal of Climate*, 19(11), 2617-2630.
- Qu X, Hall A (2007) What controls the strength of snow-albedo feedback? *Journal of Climate*, 20(15), 3971-3981.
- Qu X, Hall A (2014) On the persistent spread in snow-albedo feedback. *Climate dynamics*, 42(1-2), 69-81.
- Riggs GA, Hall DK, Salomonson VV (2006) MODIS snow products user guide to collection 5. Digital Media, 80, 6, 1-80.
- Robinson DA, Kukla G (1984) Albedo of a dissipating snow cover. *Journal of Climate and Applied Meteorology*, 23(12), 1626-1634.

- Robock A (1980) The seasonal cycle of snow cover, sea ice and surface albedo. *Monthly Weather Review*, 108(3), 267-285.
- Rossow WB, Schiffer RA (1999) Advances in understanding clouds from ISCCP. *Bulletin of the American Meteorological Society*, 80(11), 2261-2287.
- Schaaf CB, Gao F, Strahler AH, Lucht W, Li X, Tsang T et al (2002) First operational BRDF, albedo nadir reflectance products from MODIS. *Remote sensing of Environment*, 83(1), 135-148.
- Šeparović L, Alexandru A, Laprise R, Martynov A, Sushama L, Winger K et al (2013) Present climate and climate change over North America as simulated by the fifth-generation Canadian regional climate model. *Climate Dynamics*, 41(11-12), 3167-3201.
- Solomon S, Qin D, Manning M, Chen Z, Marquis M, Averyt KB et al (2007) Climate change 2007-the physical science basis: Working group I contribution to the fourth assessment report of the IPCC, Cambridge University Press, 4, 996.
- Şorman AÜ, Akyürek Z, Şensoy A, Şorman AA, Tekeli AE (2007) Commentary on comparison of MODIS snow cover and albedo products with ground observations over the mountainous terrain of Turkey. *Hydrology and Earth System Sciences*, 11(4), 1353-1360.
- Stamnes K, Tsay SC, Wiscombe W, Jayaweera K (1988) Numerically stable algorithm for discrete-ordinate-method radiative transfer in multiple scattering and emitting layered media. *Applied Optics*, 27(12), 2502-2509.
- Stroeve JC, Box JE, Haran T (2006) Evaluation of the MODIS (MOD10A1) daily snow albedo product over the Greenland ice sheet. *Remote Sensing of Environment*, 105(2), 155-171.
- Sundqvist H, Berge E, Kristjánsson JE (1989) Condensation and cloud parameterization studies with a mesoscale numerical weather prediction model. *Monthly Weather Review*, 117(8), 1641-1657.

- Thackeray CW, Fletcher CG (2016) Snow albedo feedback current knowledge, importance, outstanding issues and future directions. *Progress in Physical Geography*, 10, 1177.
- Taylor KE, Stouffer RJ, Meehl GA (2012) An overview of CMIP5 and the experiment design. *Bulletin of the American Meteorological Society*, 93(4), 485-498.
- Uppala SM, Kallberg PW, Simmons AJ, Andrae U, Bechtold VD, Fiorino M et al (2005). The ERA-40 re-analysis. *Quarterly Journal of the Royal Meteorological Society*, 131(612), 2961-3012.
- Verseghy DL (2009) CLASS-The Canadian Land Surface Scheme (Version 3.4), technical documentation (Version 1.1). Internal report, Climate Research Division, Science and Technology Branch, Environment Canada, 183.
- Wang L, Mackay M, Brown R, Bartlett P, Harvey R, Langlois A (2014) Application of satellite data for evaluating the cold climate performance of the Canadian Regional Climate model over Québec, Canada. *Journal of Hydrometeorology*, 15(2), 614-630.
- Wanner W, Li X, Strahler AH (1995) On the derivation of kernels for kernel-driven models of bidirectional reflectance. *Journal of Geophysical Research: Atmospheres* (1984–2012), 100(D10), 21077-21089.
- Zadra A, Caya D, Côté J, Dugas B, Jones C, Laprise R et al (2008) The next Canadian regional climate model. *La Physique au Canada*, 64(2), 75-83.
- Zadra A, McTaggart-Cowan R, Roch M (2012) Recent changes to the orographic blocking. Seminar presentation, RPN, Dorval, Canada, 30 March 2012. [http://collaboration.cmc.ec.gc.ca/science/rpn/SEM/dossiers/2012/seminaires/2012-03-30/Seminar\\_2012-03-30\\_Ayrton-Zadra.pdf](http://collaboration.cmc.ec.gc.ca/science/rpn/SEM/dossiers/2012/seminaires/2012-03-30/Seminar_2012-03-30_Ayrton-Zadra.pdf). Accessed 19 July 2012
- Zadra A, Roch M, Laroche S, Charron M (2003) The subgrid-scale orographic blocking parametrization of the GEM Model. *Atmosphere-ocean*, 41(2), 155-170.

Zhang Y, Rossow WB, Lacis AA, Oinas V, Mishchenko MI (2004) Calculation of radiative fluxes from the surface to top of atmosphere based on ISCCP and other global data sets: Refinements of the radiative transfer model and the input data. *Journal of Geophysical Research: Atmospheres* (1984–2012), 109(D19), D19105.